Modeling the Role of the Alpha Rhythm in Attentional Processing during Distractor Suppression

Mauro Ursino

Abstract

■ Recent experimental results suggest that alpha oscillations in brain neuroelectrical activity do not merely represent an idling phenomenon but actively participate in attention to suppress distractors and reduce cognitive workload. However, the exact mechanism responsible for this attentional processing is still a matter of research. In this work, we propose a simple mechanism for distractor suppression using a neural mass model of oscillating, interconnected cortical regions, based on alpha oscillations and their interaction with the gamma rhythm. Essentially, the model distinguishes between certain "sensory" areas, where stimuli are coded and represented via gamma oscillations, a downstream "detection" area dedicated to processing these stimuli, and a "control" region that generates the alpha rhythm. Unattended stimuli in a sensory area can be suppressed by simply imposing an alpha rhythm that is out of phase compared with the detection layer. A sensitivity analysis performed on a simple paradigmatic model emphasizes the robustness of the proposed mechanism versus parameter changes. Moreover, a more complex example (concerning spatial attention, where objects are represented through a Gestalt proximity rule) supports the capacity of the mechanism to suppress distractors in multi-unit networks. The model aligns with several experimental results and can be further utilized to investigate cognitive alterations in pathological conditions, such as schizophrenia, characterized by dysfunction in the gamma rhythm. ■

INTRODUCTION

The selection of data from the external environment is crucial in many cognitive tasks to prevent information overload and improve the efficiency of the processing stream. This *selective attention mechanism* can involve enhancing the responsiveness of neurons that process relevant targets and inhibiting unessential distractors (Schneider, Herbst, Klatt, & Wöstmann, 2022; Foxe & Snyder, 2011).

In recent years, a large quantity of data emphasized that brain oscillations play a pivotal role in selective attention, with particular consideration on the alpha rhythm (8–12 Hz) and its engagement with the gamma rhythm (>30 Hz). A broadly shared assumption is that the γ-activity mainly reflects bottom–up communication (from primary areas to higher areas), and the α-rhythm is a top–down control (Fries, 2015).

An influential hypothesis (Klimesch, 2012) assumes that an increase in the alpha activity does not simply represent a "cortical idling," as traditionally believed (Pfurtscheller, Stancák, & Neuper, 1996), but it actively implements inhibition of neural pathways unessential for the task, thus realizing an attentional suppression mechanism that disregards unattended objects or features. Support for this hypothesis comes from EEG and magnetoencephalography experiments, showing that alpha activity increases over task-irrelevant groups of neurons, alpha power decreases (event-related desynchronization) in cortical regions contralateral to a target, and alpha power increases (event-related synchronization) in the cortical areas contralateral to a distractor (Bacigalupo & Luck, 2022; van Diepen, Foxe, & Mazaheri, 2019; Wöstmann, Alavash, & Obleser, 2019; Janssens, De Loof, Boehler, Pourtois, & Verguts, 2018; Wildegger, van Ede, Woolrich, Gillebert, & Nobre, 2017; Ikkai, Dandekar, & Curtis, 2016). Moreover, this hemispheric alpha lateralization is correlated with subsequent behavioral performance (Bonnefond & Jensen, 2012; Busch, Dubois, & VanRullen, 2009). An inverse relationship has been observed between visual stimulus detection ability and power over occipital cortex (van Dijk, Schoffelen, Oostenveld, & Jensen, 2008; Ergenoglu et al., 2004), whereas lower alpha power is associated with false alarms (Iemi, Chaumon, Crouzet, & Busch, 2017; Limbach & Corballis, 2016). Finally, recent data suggest that alpha-band suppression works not only to implement endogenous (voluntary) attention but also during the involuntary capturing by salient external stimuli (i.e., exogenous attention; Arana et al., 2022).

Further results suggest that not only the amplitude but also the phase of the alpha rhythm is essential; manipulation of the alpha phase results in poor performance (Hülsdünker, Strüder, & Mierau, 2018; Bonnefond & Jensen, 2012, 2013, 2015; Busch et al., 2009) and substantially impacts stimuli detection or suppression (Harris, Dux, & Mattingley, 2018), although some critical opinions can also

University of Bologna

Journal of Cognitive Neuroscience 37:12, pp. 2469–2492
https://doi.org/10.1162/JOCN.a.65

be found on this point (Ruzzoli, Torralba, Morís Fernández, & Soto-Faraco, 2019; van Diepen & Mazaheri, 2018; van Diepen, Cohen, Denys, & Mazaheri, 2015).

Despite the large consensus on the alpha "gating by inhibition mechanism" (but see also Foster & Awh, 2019, for a different opinion), the neural bases by which alpha oscillations prevent the processing of unattended stimuli remain a matter of active debate. In this context, mechanistic neurocomputational models can provide essential indications to accept or reject hypotheses, formulate new theories, and provide testable predictions. Indeed, significant modeling contributions appeared recently to underline the role of alpha modulation in attention and its relationship with the gamma rhythm.

In the "inhibition timing hypothesis," Klimesch (2012) suggests that both an increase in alpha amplitude and a change in baseline allow for different inhibition of the gamma rhythm, depending on the excitation level of target cells, thereby implementing suppression in task-irrelevant networks. In a similar recent theorization proposed by Zazio, Schreiber, Miniussi, and Bortoletto (2020), named "the oscillation-based probability of response," the alpha-modulated gamma oscillations determine the probability of responding to a stimulus for neurons in sensory areas. The model allows the computation of a psychometric curve.

Other recent models emphasize the role of the phase in alpha oscillations, together with its amplitude (Bonnefond, Kastner, & Jensen, 2017; Quax, Jensen, & Tiesinga, 2017). For example, in a mechanism proposed by Jensen, Gips, Bergmann, and Bonnefond (2014) and Jensen, Bonnefond, and VanRullen (2012), the amplitude of alpha activity affects the duty cycle and determines how many neuronal representations can be processed per alpha period, with the more salient features appearing at an earlier phase of the alpha. Hence, in this model, competing representations are activated at different phases of the alpha cycle. A different approach has been proposed by Lundqvist, Herman, and Lansner (2013), who used an attractor network that spontaneously exhibits an alpha rhythm and switches to a gamma rhythm when a stimulus is detected. Via simulations, the authors demonstrated that both the amplitude and the phase of the alpha rhythm modulate the transition probability.

Two recent contributions also emphasize the alpha phase's role, offering a convincing mechanistic interpretation. Quax and colleagues (2017) developed a computer model of two interconnected regions, each comprising inhibitory and excitatory neurons, that oscillated with a gamma rhythm, and studied the information transmission between them as a function of an external alpha drive. Results show that the phase of the alpha drive plays a relevant role in affecting communication in terms of the coherence between the two gamma. A further excellent analysis of how communication between brain areas can be implemented via gamma oscillations nested within alpha oscillations is provided by Bonnefond and colleagues (2017). The authors' basic idea is that gamma oscillations reflect the between-areas communication, whereas the amplitude and phase of the alpha drive, modulated locally on a fine scale, control this communication. In particular, to prevent the transfer of information, alpha oscillations in one area must be asynchronous with those in another area.

Building on the ideas presented by Bonnefond and colleagues (2017), this study develops a new, more comprehensive neurocomputational model of gamma oscillations nested within the alpha cycle, which realizes powerful gating through inhibition. We propose an original mechanism based on synapse modulation that can completely suppress any uninfluential gamma oscillation in downstream areas (where the stimuli are processed), maintaining the flexibility to process the same stimulus in other areas. The mechanism works by modifying a connectivity parameter linking the alpha drive to the sensory region. Physiologically, this may be achieved through neuromodulation, for example, by an acetylcholine effect on synapses (Hasselmo & Giocomo, 2006).

To realize such a network, we used neural mass models developed in previous years (Ursino, Cesaretti, & Pirazzini, 2023; Cona, Zavaglia, Massimini, Rosanova, & Ursino, 2011; Ursino, Cona, & Zavaglia, 2010), in which oscillations emerge due to feedback among excitatory and inhibitory local populations.

First, we present a simple network with only four columns (the alpha rhythm, two sensory units oscillating with the gamma rhythm, and one downstream unit that processes the stimuli) to show the main principles of the model. In this simple case, a sensitivity analysis is performed to test the range of robustness for the parameters. Subsequently, the same mechanism is implemented to realize selective attention in a more realistic task concerning spatial attention (i.e., stimulus suppression in unattended areas).

Finally, several results in the literature suggest that the gamma rhythm is impaired in some neurological disorders (especially schizophrenia; Senkowski & Gallinat, 2015) mainly because of a defect in the development and function of inhibitory interneurons (Lewis, Curley, Glausier, & Volk, 2012; Marín, 2012). Accordingly, we tested model behavior in conditions of reduced connectivity from fast gamma-aminobutyric acid (GABA)ergic interneurons within cortical columns. Results show that deficits in selective attention arise due to interneuron dysfunction, paralleling results in the literature. This opens some perspectives for the comprehension of attention deficits in neurological disorders.

METHODS

The following section provides a qualitative description of the models used in this work, emphasizing the primary mechanisms underlying alpha–gamma coupling, communication by coherence, and gating by alpha inhibition. First, the model of a single cortical column is introduced

in the Model of a Cortical Column section. Then, a straightforward schema, which includes just four cortical columns (one for alpha rhythm generation, two for the representation of antagonistic stimuli, and the latter for detection and selection), is introduced in The Basic Model section to demonstrate the main model's working principles. Finally, A Model for Selective Spatial Attention section describes a more complex model devoted to a spatial selection task in which objects are perceived and selected based on Gestalt proximity.

The Appendix provides a more detailed description of the models, including equations and numerical values of the parameters.

Model of a Cortical Column

In the following, the terms "Cortical Column" and "Computational Unit" are considered synonymous and will be referred to collectively as "Unit." The model of each Unit, representing a cortical column, consists of the feedback connection among a population of pyramidal neurons, a population of excitatory interneurons (both using glutamatergic synapses), a population of GABAergic inhibitory interneurons with slow synapse dynamics, and a population of GABAergic inhibitory interneurons with fast synapse dynamics (see Figure A1 in the Appendix). As traditionally done in neural mass models (see Bensaid, Modolo, Merlet, Wendling, & Benquet, 2019; Cona & Ursino, 2015; Wendling, Bartolomei, Bellanger, & Chauvel, 2002; Jansen & Rit, 1995), a population consists of a group of neurons of the same kind, which share similar inputs and exhibit similar global dynamics; hence, they are represented through a collective quantity. In particular, the output of each population represents their spike density, whereas another important quantity, more similar to EEG, is the postsynaptic potential in the pyramidal population. More details on the construction of individual computational units can be found in previous articles by the authors (Cona & Ursino, 2015; Cona et al., 2011; Ursino et al., 2010), as well as in the Appendix, where all equations and numerical parameter values are provided.

Depending on the parameters that describe the internal connectivity weight and time constants, cortical units can oscillate at different rhythms (see also Ricci, Magosso, & Ursino, 2021). In this work, as described in the Appendix, parameters have been chosen to generate a rhythm either in the alpha or gamma band. In particular, we assumed that the synapse time constants are moderately higher in the α-region than in the γ-region, and more importantly, the α-region exhibits much stronger connectivity from slow inhibitory interneurons to pyramidal neurons. In contrast, the γ-region exhibits stronger connectivity from pyramidal neurons to fast-inhibitory interneurons. More particularly, in our model, the generation of the gamma rhythm depends on two simultaneous feedback mechanisms: the interaction between excitatory pyramidal and fast GABAergic interneurons (with global feedback gain C_{fp}. C_{pf} in Figure A1 of the Appendix), a mechanism also named PING in the literature (Viriyopase, Memmesheimer, & Gielen, 2016), and an inhibitory autoloop among fast inhibitory interneurons (with gain C_{ff} in Figure A1), a mechanism also named ING. Hence, the role of slow inhibition is more significant in the α-region, and the role of fast inhibition prevails in the γ-region.

Cortical units can be connected via long-range synapses. It is well known that long-range synapses in the brain are realized by axons of pyramidal glutamatergic neurons (Gerfen, Economo, & Chandrashekar, 2018). However, as demonstrated in the Results section and discussed in the final section, a balance between excitation and inhibition is necessary to achieve robust synchronization among different Units in the gamma band (Salkoff, Zagha, Yüzgeç, & McCormick, 2015; Ursino, Magosso, & Cuppini, 2009; Hasenstaub et al., 2005). In particular, excitatory links can produce excessive activity spreading across a network, causing some units to reach saturation. Hence, long-range inhibitory connections are necessary to control the global level of gamma oscillations in the net. Accordingly, we assumed that pyramidal neurons in each unit could send both long-range connections to pyramidal postsynaptic neurons in other units (thus realizing an excitatory "pyramidal – pyramidal" link) and long-range connections to postsynaptic fast-inhibitory interneurons in other units (thus realizing a disynaptic inhibitory link, "pyramidal – fast inhibitory – pyramidal"). In the following, the first connections will be generically referred to as "excitatory" and represented by the connection strength W^{ex}. In contrast, the second connection will be referred to as "inhibitory" and will be defined by the connection strength, W^{in}. A qualitative example of the connectivity between two units is illustrated in the bottom columns of Figure A1 in the Appendix (Figure A1B and C).

The Basic Model

The simplest version of our model is illustrated in Figure 1A. It consists of four cortical computational units. Units 1 and 2 (referred to as sensory units) receive external sensory input and Gaussian noise and, if excited, oscillate independently in the gamma band. Due to noise, these oscillations are generally out of phase. Unit 3 receives a constant input and Gaussian noise, generating a rhythm in the alpha band. This Unit can be located in the thalamus or pFC, as discussed in the last section. If the thalamus produces the alpha wave, it might also play a bottom–up role, as suggested in the literature (Karvat & Landau, 2024; Alamia, Timmermann, Nutt, VanRullen, & Carhart-Harris, 2020) and might also be involved in exogenous attention (Arana et al., 2022). Finally, parameters in Unit 4 (named *Detection Unit*) are the same as in Units 1 and 2 (hence, this Unit produces an intrinsic rhythm in the gamma band). However, this receives only external noise and remains silent, with only negligible activity, unless stimulated through the connectivity from the sensory units. This

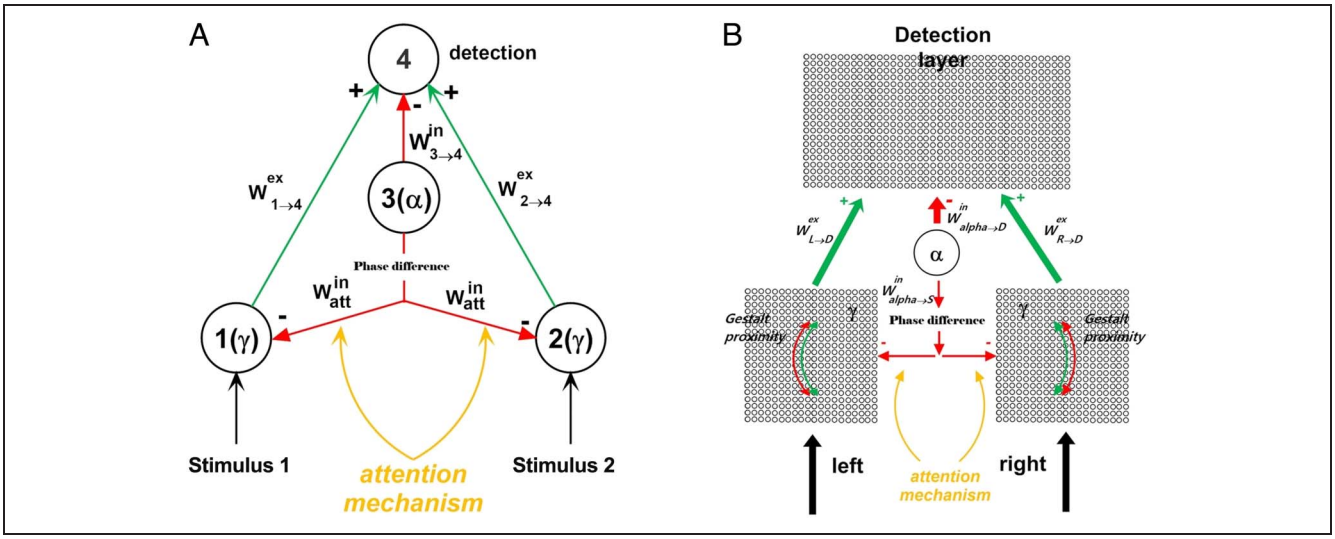

Figure 1. Block diagram of the two models used in this work. Each Unit (described through an open circle) has been implemented with the cortical column model shown in Appendix Figure A1. Green lines represent glutamatergic excitatory synapses linking pyramidal neurons in the presynaptic Unit to pyramidal neurons in the postsynaptic Unit. Red lines indicate glutamatergic synapses connecting pyramidal neurons in the presynaptic Unit to fast-inhibitory interneurons in the postsynaptic Unit, hence with an inhibitory function. In both models, the alpha rhythm is generated by a single specialized Unit and transmitted to all Units in the detection (reconstruction) layer, and, under attention, to specific Units in the perception layer that code for distractor stimuli. (A) Basic model consisting of just four Units. Units 1 and 2 are sensory elements oscillating with the gamma rhythm; Unit 3 is an alpha oscillator. Unit 4 oscillates in the gamma frequency but also receives the alpha rhythm from 3. The attention mechanism sets the value of synapses from Unit 3 to the sensory units. A high value of this synapse (with a 180-degree phase difference) results in suppression of the corresponding stimulus in Unit 4. (B) Model implemented to simulate spatial attention, with a layer simulating a portion of the left hemispace, a layer simulating a part of the right hemispace, and a detection layer. The meaning of symbols is similar as in (A), but now each layer consists of a regular lattice of neurons, oscillating with the gamma frequency, each coding for a spatial position. Moreover, proximal neurons are connected through excitatory and inhibitory synapses, which decrease with distance, implementing a proximity Gestalt rule.

Unit can represent an upper area specialized in stimulus detection.

The Units are connected according to the feedforward schema shown in Figure 1A. Units 1 and 2 send constant excitatory connectivity to Unit 4, thus transmitting their gamma oscillations downstream. If no other mechanism is included (see the Results section), Unit 4 detects the activity of Units 1 and 2 and reproduces the superimposition of the same oscillatory patterns. More clearly, the activities of Units 1 and 2 are passed through glutamatergic synapse dynamics, and these postsynaptic potentials are summed. Then, the final postsynaptic potential of pyramidal neurons in Unit 4 is passed through a sigmoidal relationship. This sigmoidal relationship performs detection. If the potential is too small, the sigmoidal output is negligible, meaning the stimulus is effectively ignored. The "gating by inhibition" mechanism and the "alpha–gamma coupling" result from the activity in Unit 3, which is transmitted to the other units. In particular, we assume that Unit 3 sends constant inhibitory connectivity (i.e., an excitation directed to fast GABAergic interneurons) to Unit 4, imposing its alpha rhythm on the latter. As a consequence, Unit 4 can detect a stimulus only during half of the alpha period (approximately 50 msec). Conversely, the connectivity from Unit 3 to Units 1 and 2 (i.e., from the alpha generator to the sensory units, but with approximately a 180-degree phase difference compared with the 3→4 alpha wave) can be variable and controlled by attention. This can occur as a consequence of neuromodulation, for instance, mediated by changes in acetylcholine concentration. The main points (to be validated in the Results section) are as follows:

i) If no signal is sent from Unit 3 (alpha generator) to a sensory unit (either Unit 1 or Unit 2), the latter oscillates in the gamma range, and this stimulus is entirely detected by the Detection Unit 4, resulting in an α-γ superimposition;
ii) selectivity attention works as follows: If Unit 3 sends a signal (with approximately a 180-degree phase difference with respect to the 3→4 alpha signal) to the fast GABAergic population in a sensory unit (Unit 1 or Unit 2), the corresponding sensory unit oscillates with a gamma + alpha coupling, but, due to phase opposition, its activity becomes unable to affect the Unit 4 (i.e., it is gated by the alpha rhythm). In other words, the sensory unit is active only during half of the alpha rhythm when the detection unit is "blind." It is worth noting that, in this condition, alpha power appears in the suppressed sensory region, as a marker of inhibition (i.e., an increase in alpha amplitude is observed in the unattended area in accordance with the experimental data mentioned above).

To realize the gating by inhibition described in point (ii), the alpha rhythm received by sensory units (1 or 2) must be in phase opposition compared with the rhythm

received by Unit 4, that is, the 3→4 alpha wave. (See the sensitivity analysis in the Results section to demonstrate this point.) The latter assumption agrees with previous observations (Bonnefond et al., 2017; Quax et al., 2017). Moreover, it is worth noting that the gating mechanism does not work correctly if the alpha rhythm is transmitted via excitatory synapses to pyramidal neurons. Still, it must target the GABAergic fast interneurons (see the Results section). In other words, it works through inhibition.

A list of parameters for the model in Figure 1A can be found in the Appendix.

A Model for Selective Spatial Attention

The abovementioned mechanism has been tested in a more sophisticated scenario, implementing spatial selection between the left and right hemispaces. To this end, we consider, instead of a single Unit 1 in the previous model, a regular lattice of 10 × 10 units representing a portion of the left space (denoted "Left layer" in the following; see Figure 1B) and, instead of Unit 2, a regular lattice of other 10 × 10 Units representing a portion of the right space ("Right layer" in the following). Each Unit of these two lattices sends a single excitatory connection to a corresponding unit in a lattice with dimension 10 × 20 (named "Detection layer," which plays the same role as Unit 4 in the previous schema) devoted to detecting stimuli in both the left and right spaces. Finally, the single Unit 3, which implements the alpha rhythm, sends an inhibitory connection to all units in the "Detection layer" and a variable inhibitory connection (with a 180-degree phase difference, i.e., out of phase), under attention

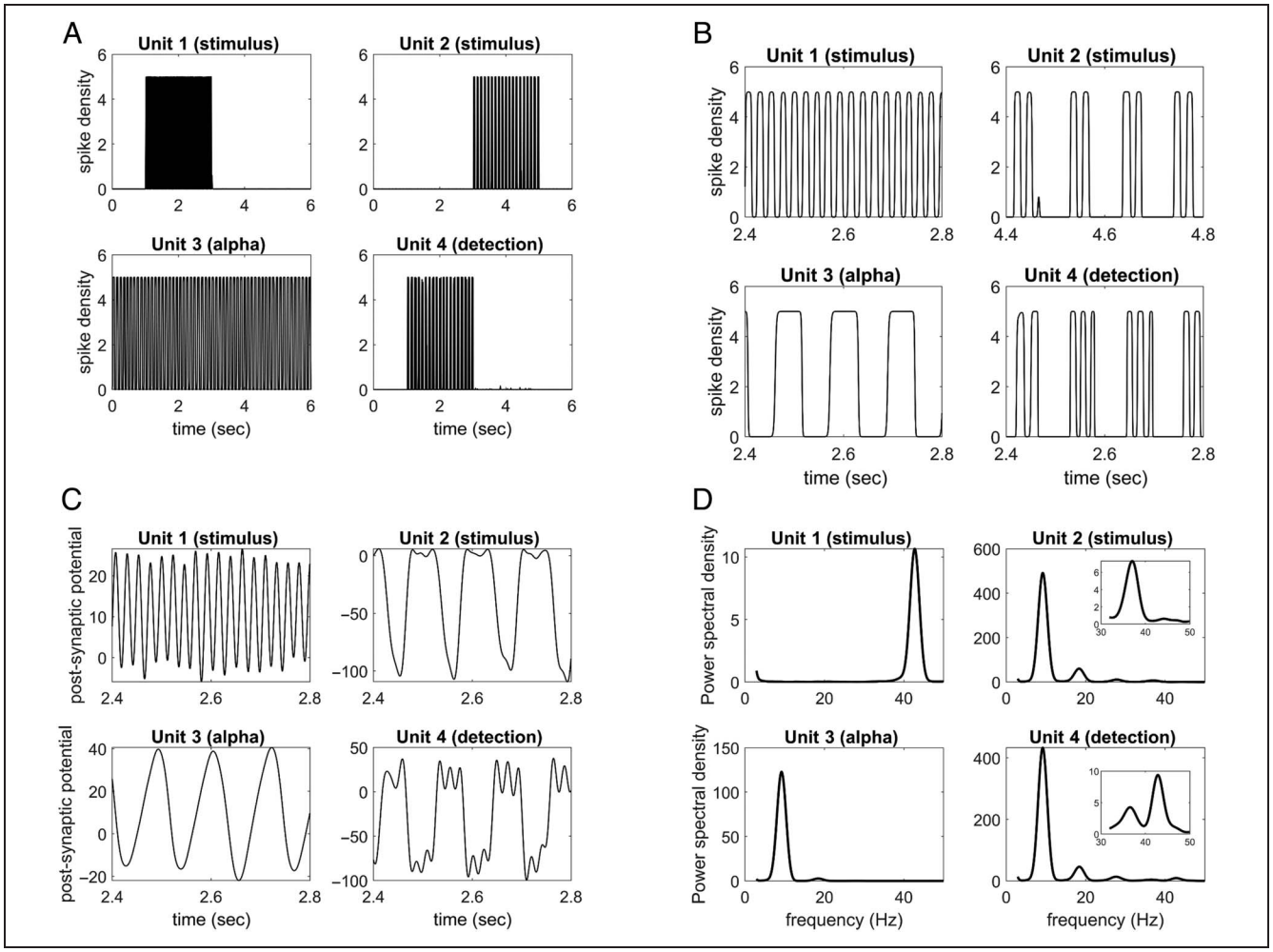

Figure 2. Simulation of the basic model (the model in Figure 1A) assuming that the Sensory Unit 1 is stimulated during the interval 1–3 sec, and the Sensory Unit 2 is stimulated between 3 and 5 sec. Unit 4 detects the stimuli. Unit 2 also receives an alpha rhythm (in phase opposition compared with the 3→4 alpha wave) from Unit 3. As a consequence, Unit 4 neglects the corresponding stimulus. (A) Temporal pyramidal neuron spike density pattern in the four Units. (B) A zoomed snapshot of pyramidal neuron spike density in all Units during a small interval of their activation. (C) A zoomed snapshot of postsynaptic potential in pyramidal neurons in all Units, showing an EEG-like pattern of their activity. (D) Power spectral density of pyramidal neuron postsynaptic potentials in the four Units. It is worth noting the α power increase in the suppressed region (Unit 2). A snapshot also shows an enlarged zoom of the gamma power in Units 2 and 4.

control, to units in the "left space" or in the "right space" to implement spatial selection.

To test the model, we considered the presence of two letters (the letter "L" in the left hemispace and the letter "C" in the right) by sending an external excitatory input to the corresponding units of the right and left layers. Our simulations demonstrate that: (i) If no alpha rhythm is imposed on these letters, both are detected in the downstream detection layer, that is, no attentive selection works. (ii) Conversely, if the alpha rhythm is transmitted to one hemispace, the corresponding letter is gated and is no longer detected in the downstream detection layer.

However, an important observation (see the Results section) is that, due to noise, the units coding for elements in the same letter oscillate in the gamma range, but with a different phase (i.e., without synchrony in the gamma band). A basic idea in the literature is that the activity of units in the same object should be synchronized to maximize the efficacy of synaptic transmission (a hypothesis known as "communication through coherence"; see Bonnefond et al., 2017; Fries, 2015). Synchronization in our model can be realized by connecting units in the "Left layer" (and in the "Right layer") through synapses that implement some Gestalt rules (Ursino, Magosso, La Cara, & Cuppini, 2006; Prodöhl, Würtz, & von der Malsburg, 2003). Notably, a more robust synchronization can be achieved using excitatory and inhibitory spatial connections because reciprocal inhibition favors synchronization (Salkoff et al., 2015; Hasenstaub et al., 2005).

In the present work, for the sake of simplicity, we implemented only the "proximity" Gestalt rule: Units that are proximal in space tend to be grouped to form a single percept. To this end, we assumed that all units in one hemispace send (and receive) excitatory and inhibitory synapses to (from) spatially proximal units. The strength of these synapses decreases with the square of the distance according to a Gaussian function (see the Appendix for mathematical details). Thanks to these "lateral synapses," units coding for the same object become synchronized in the gamma band (see the Results section).

RESULTS

Simulations with the Basic Model

Figure 2 illustrates the results of a 6-sec simulation conducted using the basic model depicted in Figure 1A. Unit 1 receives external input over the time interval of 1–3 sec, and Unit 2 receives external input over the time interval of 3–5 sec. It is worth noting that, in this simple simulation, we used two disjoint temporal intervals for the stimuli to make the inhibition more evident. The attention mechanism is set to select the first stimulus and inhibit the second by sending an alpha rhythm to Unit 2 in phase opposition compared with the 3→4 alpha phase. Figure 2A displays the spike activity of the four units. Figure 2B shows a zoomed portion of the same activity, and Figure 2C shows a zoomed portion of the pyramidal postsynaptic potentials. Figure 2D displays the corresponding power spectral density, computed using the Welch periodogram method within a 3-sec window. Unit 1 oscillates with its intrinsic gamma rhythm, whereas Unit 2 exhibits both gamma and alpha power (i.e., a significant increase in alpha power occurs in the suppressed region). Unit 3 produces the

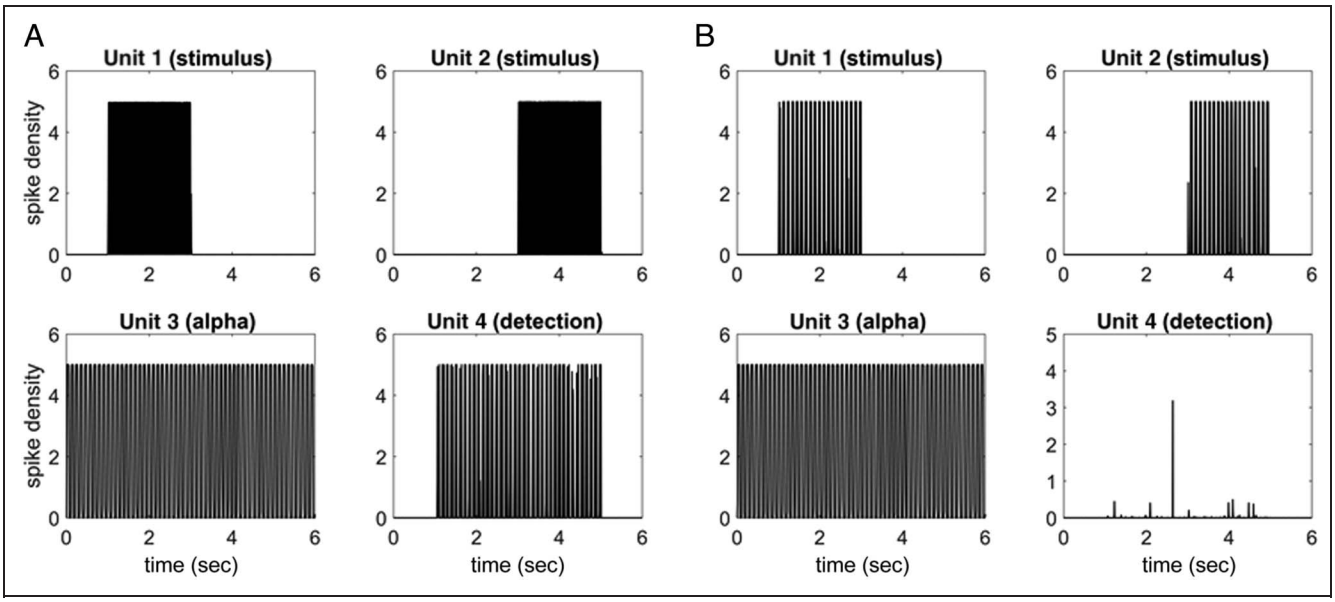

Figure 3. Simulation of the basic model (i.e., the model in Figure 1A) assuming that the Sensory Unit 1 is stimulated during the interval 1–3 sec, and the Sensory Unit 2 is stimulated between 3 and 5 sec. The plots show temporal pyramidal neuron spike density patterns in the four areas. (A) Compared with Figure 2 of the text, neither Unit 1 nor Unit 2 receives an alpha rhythm from Unit 3 for neglecting the corresponding stimulus. As a consequence, Unit 4 detects both stimuli. (B) Both Unit 1 and Unit 2 receive an alpha rhythm (in phase opposition compared with the 3→4 alpha wave) from Unit 3. As a consequence, Unit 4 neglects both stimuli.

Table 1. Sensitivity Analysis on the Connectivity Parameters in Figure 1A

$W^{ex}_{1\to4} = W^{ex}_{2\to4}$	$W^{in}_{3\to4} = W^{in}_{att}$	$W^{in}_{3\to4} = 300$ W^{in}_{att} variable	$W^{in}_{3\to4}$ variable $W^{in}_{att} = 300$	*Phase (Degree)*
≤120 undetected				
130–150 poor det.				≤130 ≥210 NO
160–460 OK	≤79 NO	≤43 NO	≤59 NO	135–150 pretty
470–660 pretty	80–87 pretty	44–53 pretty	60–75 pretty	155–185 OK
≥670 NO	≥88 OK	≥54 OK	≥76 OK	190–200 pretty

The first two columns simulate a change in the excitatory or inhibitory synapses, assuming they are equal. The third and fourth columns simulate a change in just one inhibitory synapse, maintaining the other at a constant value. Finally, the last column simulates a change in the phase difference. Parameters not indicated are held at the value shown in the Appendix.

intrinsic alpha rhythm (approximately 10 Hz) and sends it to other Units. Finally, and most importantly, Unit 4 oscillates in the alpha + gamma bands but exhibits a temporal activity only in response to the first stimulus (i.e., during the interval 1–3 sec). The response to the second stimulus (3–5 sec) is almost entirely suppressed (see the last column in Figure 2A).

It is worth noting that the two small peaks evident at about 20 and 30 Hz, in Figure 2D for Unit 2, are the second and third harmonics of the alpha rhythm, whereas a gamma peak is evident at about 37 Hz (zoomed in Figure 2D). This signifies that, compared with Unit 1, the gamma frequency moderately decreases in Unit 2 as a consequence of a nonlinear interaction with the harmonics of the alpha wave. We also show a zoomed portion of the gamma power for Unit 4, showing peaks both at 37 and 43 Hz.

If the selective mechanism is not sent to Unit 2 (nor to Unit 1), the detection unit exhibits a response to both stimuli, that is, in the overall 1- to 5-sec interval. However, if the selective mechanism is sent to both Units, the overall activity in the detection unit is suppressed. Figure 3A and B show examples of these behaviors.

To better clarify the robustness of the proposed mechanism and the main factors contributing to its functioning, we performed a sensitivity analysis on the connectivity parameters in Figure 1A, that is, on the excitatory feedforward synapses $W^{ex}_{1\to4}$ and $W^{ex}_{2\to4}$, on the feedforward inhibitory synapses $W^{in}_{3\to4}$ and W^{in}_{att}, and on the phase difference between the 3→4 and the 3→2 alpha waves. Results (Table 1) are classified as "OK" or "NO" depending on whether the selection mechanism can cancel the undesired stimulus. Furthermore, "pretty" denotes cases when a small residual of the inhibited stimulus is detected, that is, the detection mechanism works pretty well but not perfectly. Finally, the term "undetected" is used to indicate cases when the feedforward excitatory synapses cannot stimulate the detection layer. Therefore, stimuli are never detected, even in the absence of selective attention.

To assess the previous classes ("OK," "pretty," "NO," "undetected"), we used the following quantitative criteria: (i) the mean value of spike activity in the detection unit during the interval of stimulus presentation must remain below 1% of maximum to have a good stimulus suppression ("OK"); (ii) if the mean value remains below 5% of maximum but it is higher than 1%, we consider a "pretty" good suppression; (iii) if the mean activity in the detection unit is above 5% of the maximum, we consider that the attentive suppression failed ("NO"). The previous three criteria apply to the suppressed stimulus. Moreover, regarding the attended stimulus, (iv) the activity of an attended stimulus is insufficiently perceived

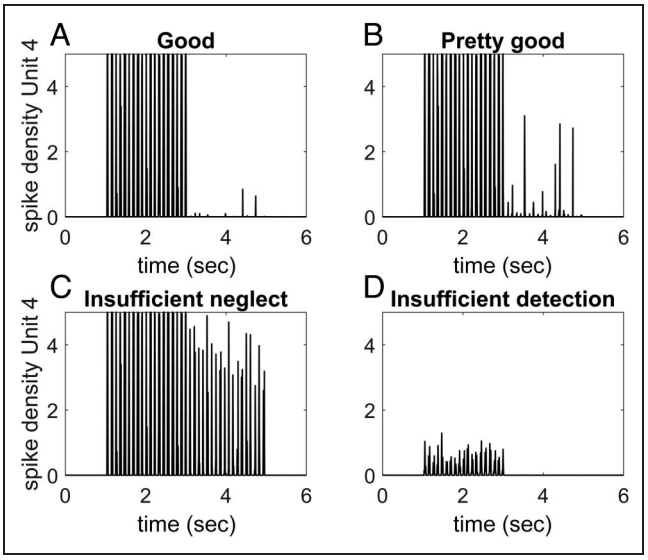

Figure 4. Simulation of the basic model (i.e., the model in Figure 1A) assuming that Sensory Unit 1 is stimulated during the interval 1–3 sec, and Sensory Unit 2 is stimulated between 3 and 5 sec, but with different parameter values. The four simulations aim to clarify the terminology used in the sensitivity analysis more effectively (see Table 1). (A) Simulation performed with $W^{in}_{3\to4} = 300$ and $W^{in}_{att} = 62$ (see the third column in Table I), providing *good* results; (B) Simulations performed with $W^{in}_{3\to4} = 300$ and $W^{in}_{att} = 52$ still providing *pretty good* results; (C) Simulation performed with $W^{in}_{3\to4} = 300$ and $W^{in}_{att} = 40$ providing an insufficient stimulus neglect; (D) Simulation performed with $W^{ex}_{1\to4} = W^{ex}_{2\to4} = 90$ (see the first column in Table 1) providing an insufficient detection of the attended stimulus. All other parameters are set to the basal value.

("undetected") if the mean value of activity during the interval is below 10% of the maximal activity. Note that when a stimulus is completely detected, the mean value of activity in Unit 4 is approximately 25% of the maximum, due to a gamma wave superimposed on an alpha wave (see Figure 2B for an example of Unit 4). Examples are provided in Figure 4 for some typical cases presented in Table 1.

Results show that the mechanism is quite robust following changes in the synapses. As expected, if the feedforward excitatory synapses are excessively decreased, the detection layer cannot detect any stimulus. Conversely, if the feedforward synapses are excessively increased (above 670), the selective attention mechanism is unable to inhibit the undesired stimulus. Regarding inhibitory synapses, there is a wide range of values for the mechanisms to function correctly. Interestingly, if one of the two synapses (either the feedforward $W^{in}_{3\to4}$ or the selective one W^{in}_{att}) is increased to 300, the other can be decreased (down to 54 or 76 in the third and fourth columns, respectively) while still maintaining proper functioning.

The only crucial parameter is the phase difference between the 3→4 and the 3→2 alpha waves. To have adequate functioning, its value must be within the interval 155–185 degrees (a larger interval of 135–200 degrees can be used to achieve pretty good, but not perfect, behavior). The possible neurophysiological mechanisms for this phase difference are discussed in the Change to Unit 3: Two Antiphase Alpha Waves and the Discussion sections.

The previous sensitivity analysis was performed with a basic phase difference as large as 165 degrees (except for the last column). A further analysis was performed, maintaining the phase shift between the alpha waves at zero and modifying the coupling strength. In this condition, the attention mechanism fails to function, even when the synapse strengths are extremely high or extremely low.

Simulation of Spatial Attention

We used the model depicted in Figure 1B to simulate a spatial attention mechanism. A letter L is presented to the left hemispace, and a letter C is presented to the right hemispace.

First, to clarify the activity in the perception layers, we show the activity in the left hemispace (stimulated as in Figure 5A) without any selective mechanism and in the absence of Gestalt lateral synapses (Figure 5B). In this condition, all units in the left hemispace representing the letter "L" oscillate with a gamma rhythm. However, they are out of phase, that is, the letter L is not perceived as a single synchronized oscillator.

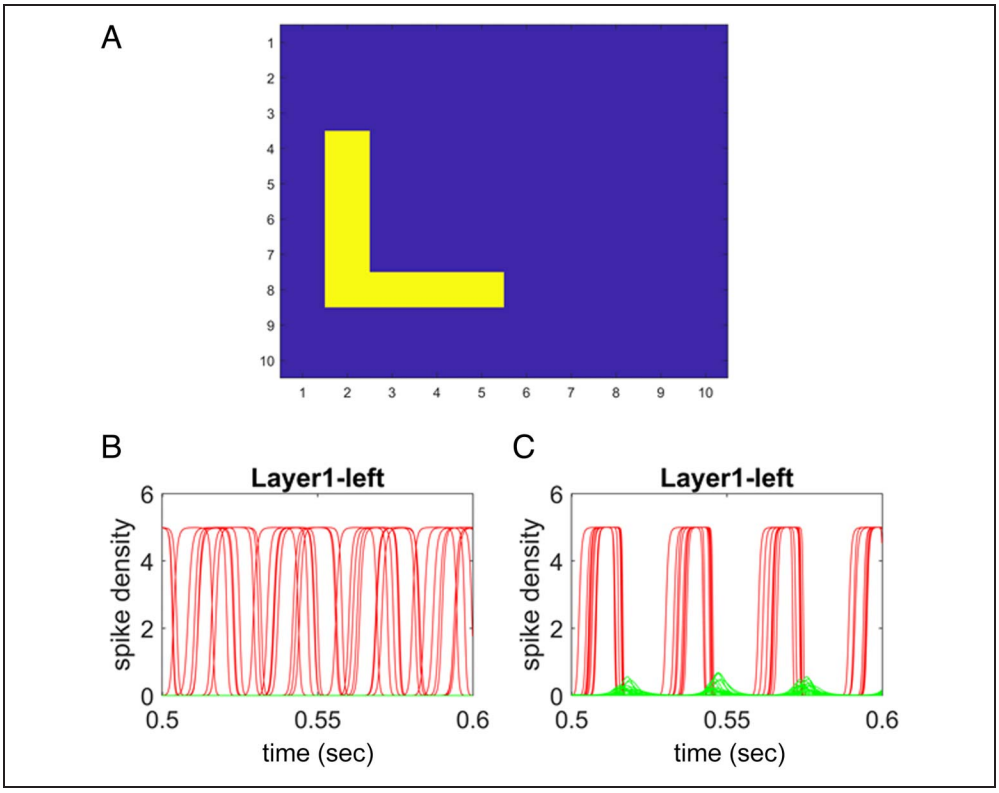

Figure 5. Simulation of the gamma rhythm for the 100 Units (10 × 10) in the layer representing a portion of the left hemispace in response to the presentation of the letter L. (A) A snapshot of the letter, where 9 Units are stimulated; (B) Temporal pattern of activity in all units, without synapses implementing the Gestalt proximity. The red lines represent the spike density of pyramidal neurons in the stimulated Units of the letter L, whereas the green lines are the spike density of nonstimulated Units. The stimulated Units oscillate with a gamma rhythm but are desynchronized in the gamma band, whereas the not-stimulated ones are silent; (C) The same simulation with lateral synapses implementing the proximity Gestalt criterion (i.e., proximal Units are linked via reciprocal synapses, whose strength decreases with distance). The Units in the letter L now oscillate in synchronism in the gamma band. A weak propagation toward proximal neurons extern of the letter is evident (as shown by mild activity in a few green lines).

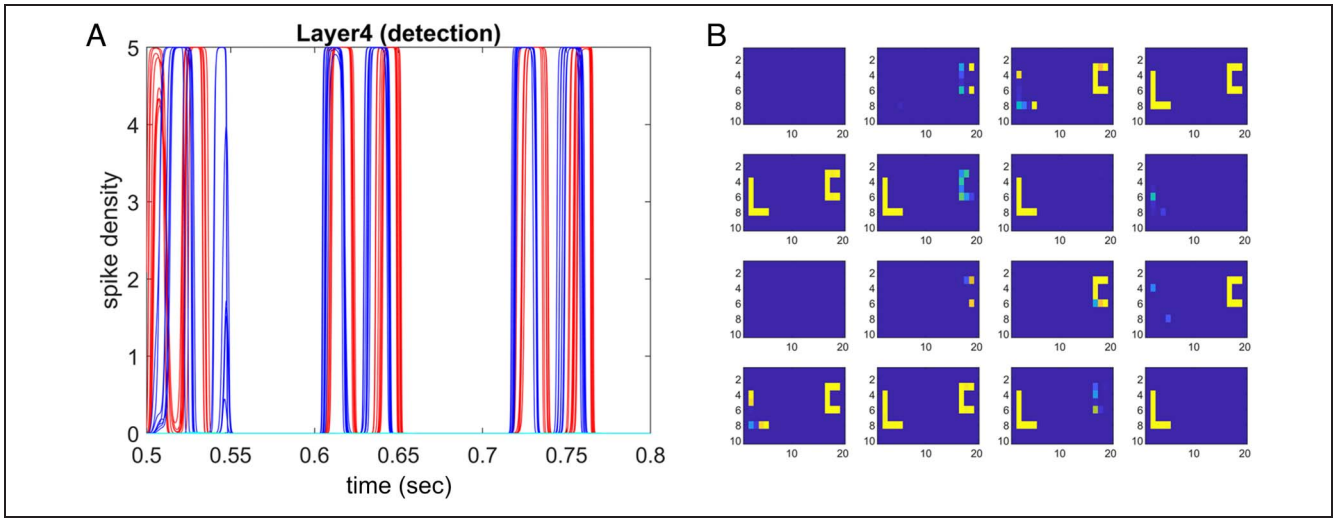

Figure 6. Simulation of the activity in the "detection layer" for the model shown in Figure 1B (spatial detection) in response to the presentation of the letter L in the left hemispace and the left C in the right hemispace. Lateral synapses implementing the Gestalt proximity criterion are used in both perception layers. No selective attention mechanism has been introduced. (A) Temporal pattern of spike density of pyramidal neurons in the Detection layer, zoomed between 0.5 and 0.8 sec. Red lines represent the activity of neurons coding for elements in the left space excited by the letter L; blue lines represent the activity of neurons coding for elements in the right space excited by the letter C; green and cyan lines denote neurons in the left and right space, respectively, which are not stimulated by any external input (hence, their activity is close to zero). Both letters are excited and oscillate with a different phase. (B) Some snapshots of the same simulations, showing activity in the overall detection layer in a small time window (approximately between 0.6 and 0.65 sec, containing two gamma peaks; the time step between two consecutive snapshots is 3 msec). Both letters in the left and right spaces are detected, and their activity is sometimes temporarily superimposed.

Then, we repeated the same simulation, implementing the Gestalt lateral synapses within the perception layer to realize a Gestalt proximity criterion. As shown in Figure 5C, all units in the letter L are now synchronized and oscillate in phase in the gamma range. Hence, Gestalt synapses are mandatory to synchronize the units representing the same letter, which otherwise would oscillate out of phase due to noise. The same, of course, is valid for the letter C in the right layer.

Starting from this condition (Gestalt proximity), we then simulated the behavior of the overall network in Figure 1B by providing the letter L as input to the left hemispace and the letter C to the right hemispace. For the sake of simplicity, we present only the oscillators belonging to the "Detection Layer" in the temporal domain (left columns in Figures 6 and 7) and some snapshots of this layer activity (right columns in Figures 6 and 7).

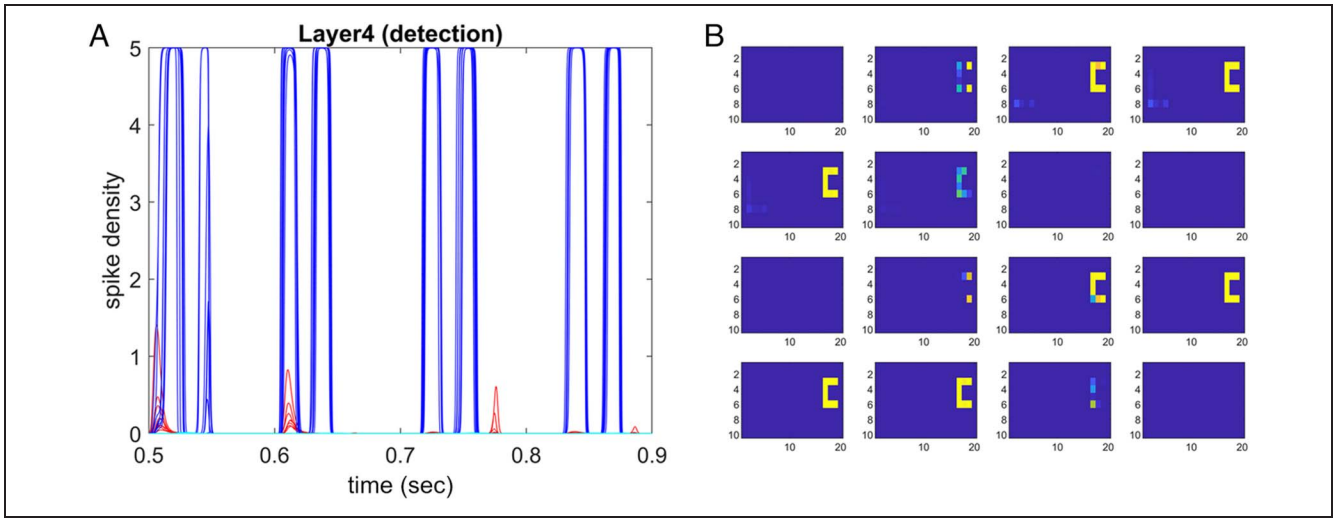

Figure 7. Spatial attention mechanism. Simulation of the activity in the "detection layer" for the model shown in Figure 1B, in response to the presentation of the letter L in the left hemispace and the left C in the right hemispace. Lateral synapses implementing the Gestalt proximity criterion are used in both perception layers. The meaning of the figures is the same as in Figure 6, but now a selective suppression mechanism (i.e., the alpha rhythm in phase opposition) has been sent to all neurons in the left hemispace. As a result, only the letter C in the right hemispace is detected, whereas the activity of neurons coding for the letter L in the left hemispace is almost eliminated.

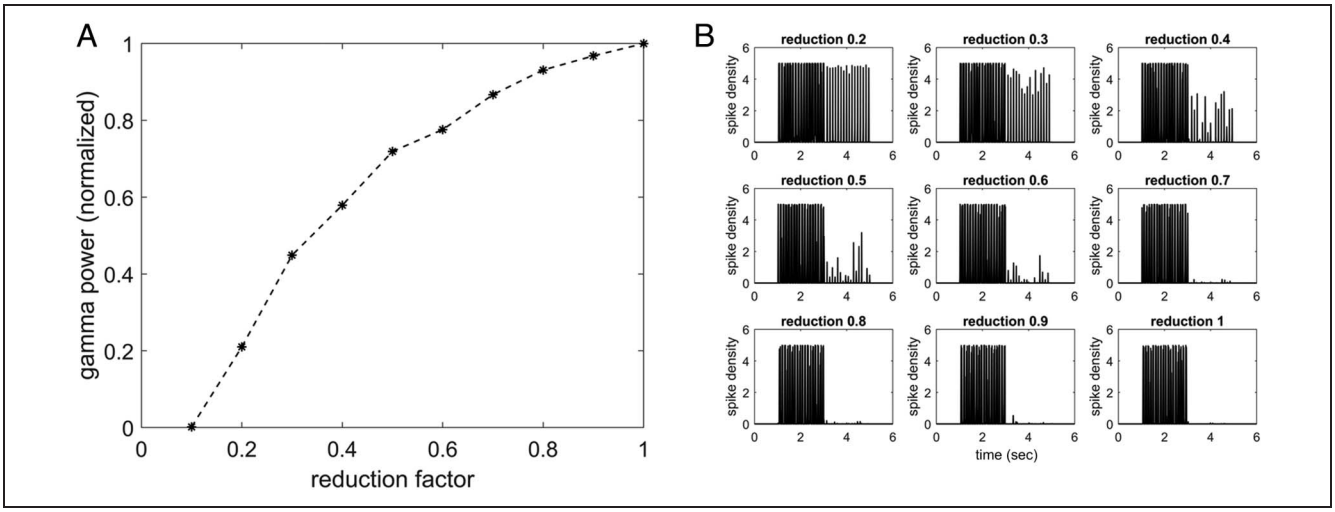

Figure 8. Simulation of the basic model (the same as in Figure 1A) with different values of the "reduction factor," which mimics a progressive reduction in the activity of GABAergic fast inhibitory interneurons. As in Figure 2, we assumed that Sensory Unit 1 is stimulated during the interval 1–3 sec, Sensory Unit 2 is stimulated between 3 and 5 sec, and moreover, Sensory Unit 2 is receiving an alpha rhythm (in phase opposition compared with the 3→4 alpha wave) from Unit 3 for neglecting the corresponding stimulus. (A) Power in the gamma band (30–45 Hz), evaluated in the Sensory Unit 1 at different reduction factor values. The power is normalized to the value obtained when GABAergic neurons work normally (i.e., when the reduction factor is as high as 1). (B) Spike density of pyramidal neurons in the detection unit for different reduction factor values. If the reduction factor falls below 0.6, the attention mechanism progressively fails to suppress the second stimulus.

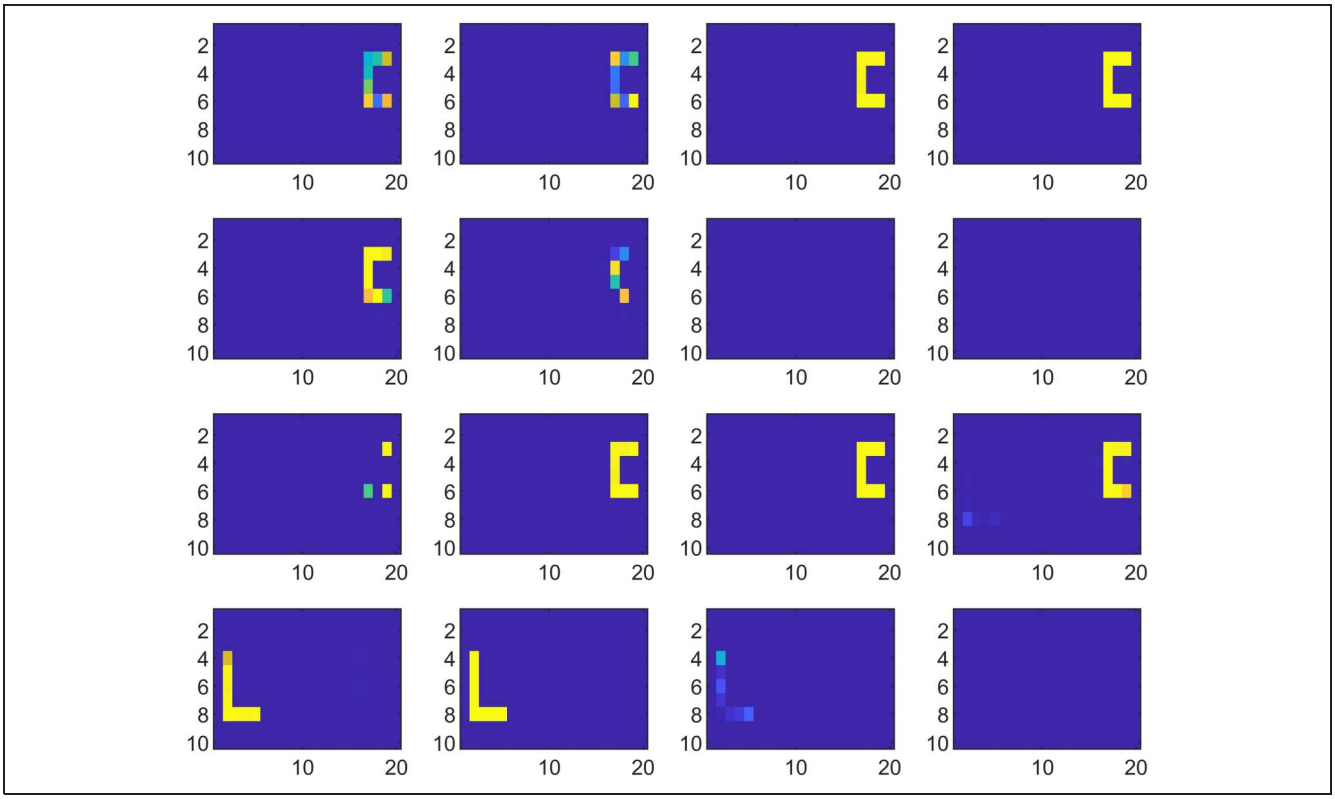

Figure 9. Spatial attention mechanism with impaired fast GABAergic interneurons. The figure shows some snapshots of the activity in the "detection layer" for the model shown in Figure 1B, in response to the presentation of the letter L in the left hemispace and the left C in the right hemispace, with a selective suppression mechanism (i.e., the alpha rhythm with approximately 180-degree phase lag) sent to all neurons in the left hemispace (this is the same simulation as in Figure 7B). However, compared with Figure 7, we now assumed a reduction factor for fast GABAergic interneurons as low as 0.3. As a result, not only is the letter C in the right hemispace detected, but also the letter L in the right space appears, denoting a failure of the attention mechanism.

Without any attentive selection (Figure 6), the units coding for both letters oscillate in the detection layer. All elements in the same letter oscillate in phase (alpha + gamma) but with a different phase compared with elements of another letter. Subsequently, we implemented the selective attention mechanism to inhibit detection in the left hemispace. To this end, we transmitted the alpha rhythm, out of phase, to all units in the left perception layer. The results (Figure 7) show that now the left portion of the detection layer is silent, and only the C letter in the right space is detected.

Simulation of a Schizophrenic Condition

Several data in the literature suggest that neurological disorders (particularly schizophrenia) are associated with a decreased activity of fast GABAergic interneurons (Lewis et al., 2012; Marín, 2012; Nakazawa et al., 2012). To test this aspect, we simulated the previous models after a reduction in the information transmitted from the fast GABAergic populations to the other populations in the cortical unit. Hence, we multiplied all the connectivity constants that exit from fast GABAergic interneurons (C_{pf}

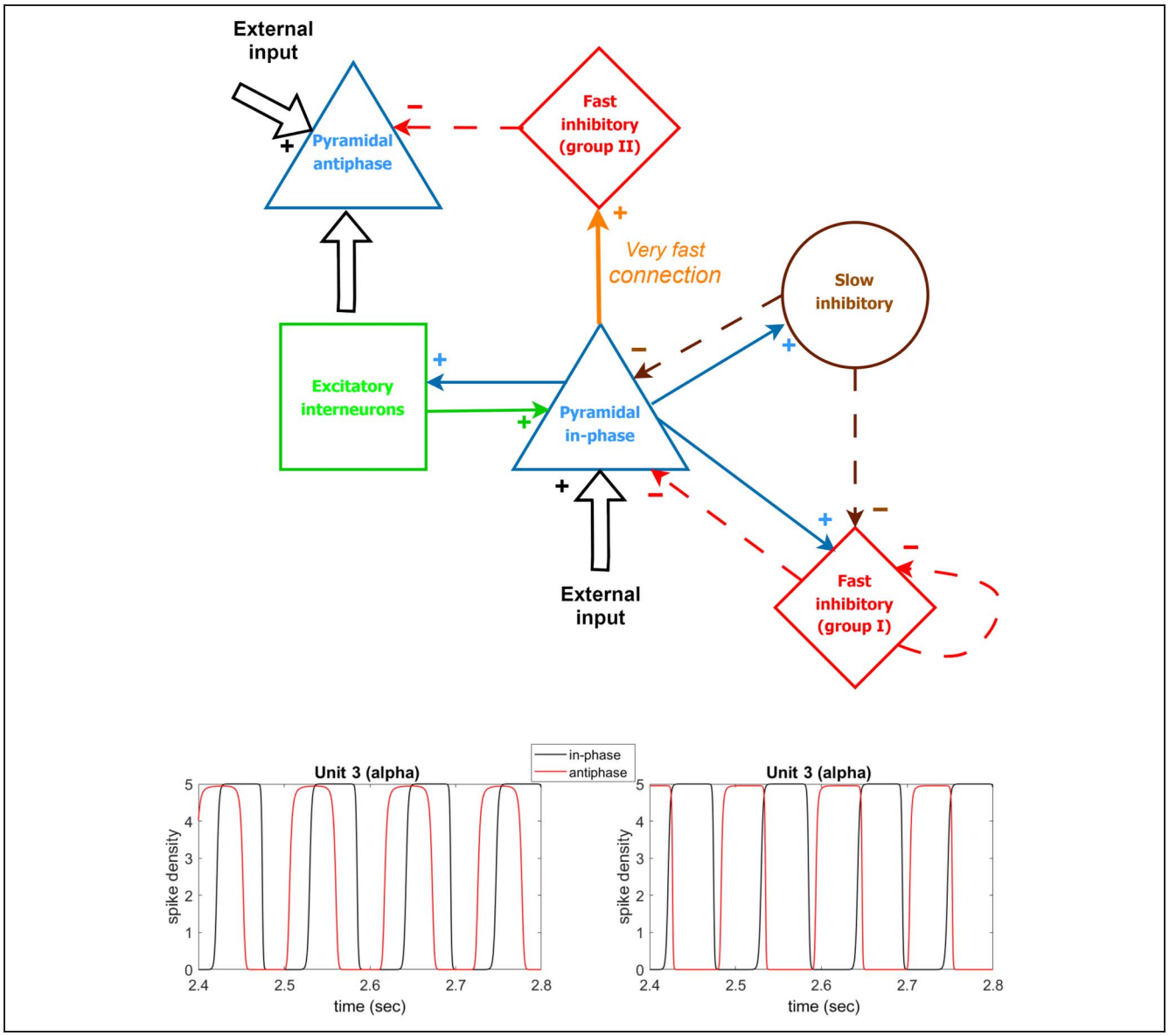

Figure 10. Upper column: schematic block diagram of Unit 3 (alpha generator), which is able to produce two alpha rhythms with a large phase shift. The large orange arrow represents a very fast excitatory connection (possibly realized using AMPA receptors), whereas the other symbols are analogous to those used in Figure A1 of the Appendix. Left bottom column: model simulations obtained using the same model as in Figure A1 of the Appendix, and assuming that the fast inhibitory population sends inhibition to a second antiphase population of pyramidal neurons. The two pyramidal populations exhibit a phase shift of approximately 90 degrees. Right bottom column: simulation obtained using the block diagram at the top of this figure (i.e., with a second population of fast inhibitory interneurons, almost instantaneously excited by pyramidal neurons). The two pyramidal populations now exhibit almost a 180-degree phase shift.

representing the connections from fast interneurons to pyramidal neurons and C_{ff} representing the auto-inhibition of fast interneurons; see Appendix and Figure A1) by a factor less than 1 (named "reduction factor" in the following). This reduction is applied similarly to all cortical units in a given model. Preliminary simulations show that, as the strength of fast GABAergic synapses is progressively reduced, the amplitude of gamma oscillations decreases. Only when this strength is reduced to 15–20% of normal does the gamma rhythm almost disappear, and the detection unit exhibits quite constant high excitation (i.e., it progressively saturates).

First, we evaluated the gamma band power in the perception layer (without the selection mechanism) when the reduction factor is progressively decreased. As evident in Figure 8A, gamma power declines due to impairment in fast GABAergic neuron activity. This result agrees with the observation of several authors (Chung, Geramita, & Lewis, 2022; Grent-'t-Jong et al., 2018; Sun et al., 2011), showing a decrease in gamma power in schizophrenic subjects. Then, we tested the effect of reducing gamma power in each of the models presented above. In each case, only the activity in the detection layer is shown for brevity.

Basic Model

As apparent in the nine columns in Figure 8B, which reproduce the same simulation as in Figure 2, a decrease in the reduction factor progressively impairs the attention mechanism, resulting in the simultaneous detection of both stimuli (the selected one, in the interval 1–3 sec, and the unattended one, in the interval 3–5 sec) if the reduction factor is decreased below 0.5–0.6.

Spatial Attention

Figure 9 shows a simulation of spatial attention performed with a reduction factor as low as 0.3. Both letters now appear (one on the left and the other on the right hemispace), that is, the selection mechanism does not work correctly to inhibit the left hemispace.

Change to Unit 3: Two Antiphase Alpha Waves

The present model requires the presence of two alpha waves, approximately in phase opposition. To enhance the reliability of our study, in this section, we present a modification of Unit 3 that can produce such behavior, utilizing two distinct populations of pyramidal neurons. We tried two different versions. First, we used the same model as in Figure A1 of the Appendix, but assuming that the fast inhibitory interneurons send further synapses to a second population of pyramidal neurons, referred to as the "anti-phase population." Hence, the first population of pyramidal neurons (referred to as the "in-phase population") inhibits the second population via a disynaptic connection, involving a glutamatergic synapse followed by a fast inhibitory GABAergic synapse. As shown in the left bottom column of Figure 10, this disynaptic connection is too slow, producing approximately a 90-degree phase difference between the alpha activity of the two populations. Hence, we propose a different model, presented in the upper column of Figure 10, where the first (in-phase) pyramidal population excites a second population of fast GABAergic interneurons via a very fast synapse. The second inhibitory population, in turn, inhibits the pyramidal antiphase population. In this way, the disynaptic connection is significantly faster and produces almost a 180-degree phase opposition between the two pyramidal populations' waves (as shown in the bottom right column of Figure 10). It is worth noting that the model in Figure 10 has not been directly used within the networks in the previous simulations and can be implemented in future works. The physiological reliability of this very fast excitatory synapse is analyzed in the discussion.

DISCUSSION

The present study proposes an original model of the alpha-suppression mechanism in attention based on oscillating neuronal masses and α-γ superimposition. The main idea is that information to be processed (for instance, a stimulus in a given spatial position) is transported by the gamma rhythm. The occurrence of a 180-degree phase shift in the alpha oscillation between two cortical areas (one devoted to stimulus perception, the other to stimulus detection and processing) allows suppression of this information in the downstream regions. Conversely, the absence of the alpha rhythm in the upstream (sensory) regions allows the maintenance of information and its subsequent processing. The mechanism is quite robust and can be implemented simply by adjusting the strength of one synapse connecting the alpha generator to the perception layer (i.e., utilizing a form of top–down control; see below).

In the following, the model's structure is first critically discussed, and then its main assumptions are checked against experimental results and neurophysiological knowledge. A comparison is made with previous theoretical work, and lines for future investigation, including testable predictions, are outlined.

Considerations on Model Structure

As demonstrated by the sensitivity analysis, inhibition is necessary for our model to establish a temporal window (lasting approximately half the alpha period) during which the detection unit is strongly inhibited and, hence, cannot detect stimuli. Moreover, the attention mechanism sends a similar inhibition, but in phase opposition, to the unattended sensory units. As a consequence, the detection unit (Unit 4 in Figure 2) is active when the sensory unit

(e.g. , Unit 2 in Figure 2) is inactive, and the detection unit is inactive when the sensory unit is active. This antiphase inhibition can be appreciated by looking at the pattern of postsynaptic potentials in Figure 2C.

It is worth noting that the present attention mechanism does not necessitate the gamma rhythm but can also work if activity in the sensory units is constant, and only modulated by the external alpha (unpublished simulations). The presence of gamma oscillations, however, makes the neuroelectrical activity in the model closer to that experimentally observed and, more importantly, can be exploited in future work to simulate conditions where different stimuli could be simultaneously detected, organized into a single percept, or separated using a gamma code. Synchronization or desynchronization of gamma oscillations can be a powerful mechanism for grouping information, facilitating optimal Hebbian learning, and distinguishing information from that of other percepts (Fries, 2009). For instance, in a recent study, Bonnefond, Jensen, and Clausner (2024) proposed that distinct gamma band bursts (>30 Hz) can be utilized within an alpha period to process distinct elements of an object separately in time.

A problem, however, as shown in Figures 2 and 6–7, is that the presence of a gamma rhythm in the model can cause perception to flicker at approximately 40 Hz. However, we think this occurs so quickly that it remains unconscious.

In the present model, the attention mechanism works by modulating the synapses from the alpha generator (Unit 3) toward the sensory units (for instance, Synapses 3→2 to attend or neglect the stimulus in Area 2). A possible objection is that a similar attentive control could be realized more directly by simply controlling the synapses exiting from the sensory units (for instance, by controlling the Synapse 2→4 to attend to or neglect the stimulus in Unit 2). However, we believe the present mechanism exhibits several advantages over the other. First, the mechanism is parsimonious compared with a possible modulation of the output synapses. Let us consider Figure 11, where we assume that some sensory units send their output signal to several different downstream areas. With the present assumption, it is sufficient to modulate one synapse entering a single Unit to transmit or neglect all its outputs. In the other hypothesis, all the output synapses exiting from that Unit should be modulated simultaneously. Second, with the proposed mechanism, it is easy to realize a spotlight that moves attention from one stimulus to another. It is sufficient to shift the reduction in synaptic strength from one point to another in Figure 11. Interestingly, in our model a stimulus is perceived by the detection unit only during a half-period of the alpha wave (approximately 50 msec; see Figure 2B). The following "blind" 50 msec could thus be used to move attention to other positions. Some authors have proposed that a spotlight attention mechanism is under frontal control and operates with a theta period (Raposo et al., 2023; Fiebelkorn & Kastner, 2019). The presence of a partial window during the alpha phase, when input stimuli are more or less efficacious, has been described in Busch and colleagues (2009).

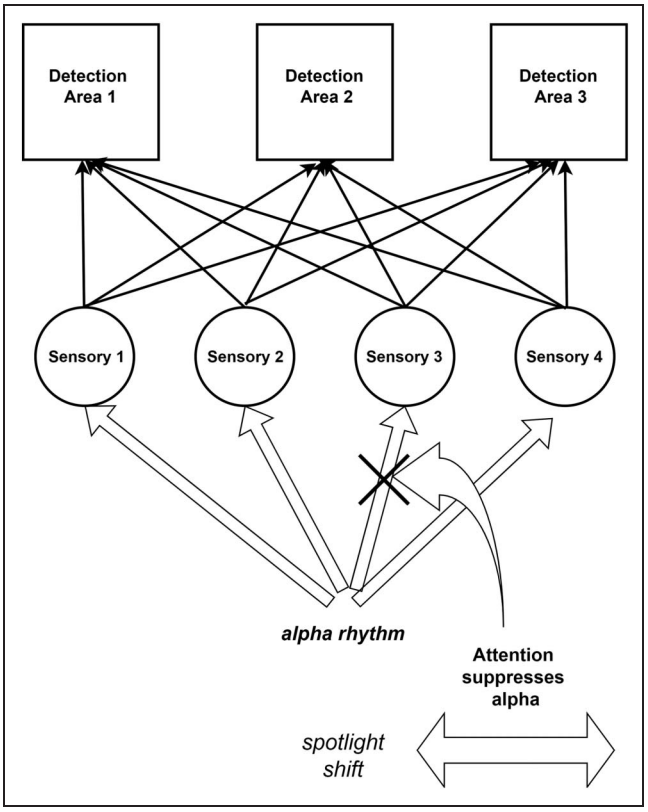

Figure 11. Block diagram illustrating how the alpha rhythm can implement a parsimonious attention mechanism by modulating an incoming synapse only. It is sufficient to suppress just one synapse entering Unit 3 to focus attention on this specific sensory stimulus and send the stimulus to various downstream detection areas by neglecting the other stimuli. Implementing a similar attention mechanism at the level of the output synapses would require that all synapses exiting from Units 1, 2, and 4 be suppressed simultaneously. Finally, it is simple to achieve a spotlight effect by moving the alpha suppression from one Unit to another.

Another important point is that the model can simulate a relaxed state or an arousal state. If alpha is decreased everywhere, all stimuli are attended (this simulates an arousal state), whereas a global increase of alpha reduces attention to the external world (relaxed state). It is well known that alpha decreases during arousal conditions and increases in a relaxed state (Barry, De Blasio, Fogarty, & Clarke, 2020; Cantero, Atienza, Salas, & Gómez, 1999).

Finally, the present mechanism can explain the experimentally observed changes in alpha amplitude in the unattended or attended areas (see Figure 2), whereas the alternative hypothesis cannot.

Throughout the present simulations, we assumed that the alpha wave produced by Unit 3 is constant and that only the synapses from Unit 3 to the sensory areas are controlled. As a consequence, Unit 4 receives a constant alpha rhythm. A more complex scenario may consider

the possibility that the rhythm in Unit 3 is directly controlled by acting on the input to this area, making the alpha wave wax and wane. This may be the subject of future work. For model functioning, it is sufficient that the alpha wave is present when the attention mechanism is operating, that is, when some unattended stimuli need to be suppressed. If the suppression mechanism is not necessary, the alpha rhythm may diminish, allowing transmission from all sensory areas to higher brain areas (arousal state). Indeed, various literature data suggest that the alpha rhythm, not only in occipital but also in frontoparietal regions, is under active top–down control (Peylo, Hilla, & Sauseng, 2021; Misselhorn, Friese, & Engel, 2019; Doesburg, Bedo, & Ward, 2016).

An essential aspect of our models is that the distractor stimulus remains present in the early sensory areas (where alpha and gamma oscillations are superimposed) and is suppressed only in higher areas dedicated to further processing. Why don't we suppress the distractor directly in the primary areas? Basically, because the stimulus is suppressed only in a top area of our model, it remains available for potential processing in other brain regions. Suppose that the sensory stimulus is sent not only to the "top" regions of our model depicted in Figure 11, but also to other regions (for instance, located in the limbic system) not included in Figure 11. Moreover, suppose that these further areas do not receive the alpha rhythm or the rhythm has a different phase there. In that case, the stimulus can be processed unconsciously in the limbic area, despite being suppressed in the top "conscious area."

Experimental Verification

Recent literature supports several aspects of the present model through experimental data. The fundamental assumption is that alpha oscillation power increases in the areas where a distractor should be neglected and decreases (becoming relatively small or negligible) in the areas where a cue must be detected for further processing. Much data align with this scenario (see Jensen et al., 2012, 2014; Klimesch, 2012, for a recent review). However, doubts have also been expressed regarding this view (Foster & Awh, 2019). Further confirmation comes from recent experiments. When a target visual stimulus is cued in the presence of a distractor, alpha power decreases over occipital cortex contralateral to the attended visual field (Ikkai et al., 2016) and increases ipsilaterally (van Diepen et al., 2019; Wildegger et al., 2017). During a flanker task, alpha power increases over visual areas processing an incongruent flanker from 300 to 500 msec poststimulus onset (Janssens et al., 2018). An analogous result occurs within the right auditory cortex: A more considerable increase in high α power occurs when attending to an ipsilateral sound and a more substantial decrease in low α power when attending to a contralateral sound (ElShafei, Bouet, Bertrand, & Bidet-Caulet, 2018). A similar mechanism also operates in multisensory conditions. For instance, alpha power is higher over visual cortex when attention is focused on the auditory part of an audiovisual stimulus (Foxe, Simpson, & Ahlfors, 1998).

A fundamental assumption of our model is that an alpha rhythm is transmitted to higher areas where the stimulus is detected and further processed. We think this assumption is physiological because much literature data confirm the widespread presence of alpha power in different cortical areas (Bourgeois, Guedj, Carrera, & Vuilleumier, 2020; Halgren et al., 2019) and provides indications that an alpha rhythm is transmitted not only toward sensory regions but also toward higher areas in the parietal and frontal regions, and in the attention network (Tabarelli, Brancaccio, Zrenner, & Belardinelli, 2022; Mishra et al., 2021; Misselhorn et al., 2019). Moreover, in the present model, the location of Unit 4 is not fixed, but it may depend on the particular task under study. The only important point is that Unit 4 is located downstream of the sensory areas to detect and process the stimulus. For instance, alpha oscillations are characteristic of attentional processes in high-level areas of the visual system (Gaillard et al., 2020; Fiebelkorn, Saalmann, et al., 2013).

Several authors debated on the origin of this ubiquitous alpha rhythm, and two main hypotheses have been formulated, one assuming a prefrontal origin, especially involving the infragranular layer of the FEF (Gaillard & Ben Hamed, 2022) and another a thalamic origin (especially the pulvinar; Bourgeois et al., 2020). Both regions have been implicated in attention control (see below). In particular, the pulvinar exhibits extensive connectivity to almost entire neocortex (Kaas & Lyon, 2007; Shipp, 2003). Some authors suggested that the pulvinar can organize cortical coherence among areas, thus modulating the transmission gain (Lakatos, O'Connell, & Barczak, 2016; Schmid, Singer, & Fries, 2012). Regarding the prefrontal hypothesis, Popov, Kastner, and Jensen (2017) observed that alpha oscillations in early visual regions reflect a feedback control exercised by the right FEF. Gaillard and colleagues emphasized the same idea, showing that a spotlight alpha rhythm, originating within the FEF, is at the source of attention control by rhythmically sampling multiple spatial positions (Gaillard et al., 2020). The present model is independent of the origin of the alpha rhythm but only assumes that this rhythm is transmitted, with a different phase, to sensory regions and higher brain areas: Both the pulvinar and the FEF can satisfy this condition.

A third necessary condition is that the alpha rhythm is actively modulated to sensory areas. Although the idea that a top–down center actively controls the alpha rhythm is commonly accepted (Gaillard & Ben Hamed, 2022; Popov et al., 2017; Quax et al., 2017; Doesburg et al., 2016), probably originating from a frontoparietal network (Mathewson et al., 2014), the exact mechanism is not outlined in the literature. Several studies have demonstrated that alpha oscillation activity is subject to internal control and can be modulated in anticipation of relevant or

distracting stimuli (Samaha, Bauer, Cimaroli, & Postle, 2015; Bonnefond & Jensen, 2012; Foxe et al., 1998). This may occur through a change in the basal value, amplitude, or phase of the alpha rhythm, or by a change in the strength of connectivity. The present model assumes the last change. As to this point, a possibility is that a neurotransmitter released as a function of the task modifies synaptic strength. For instance, acetylcholine is known to modulate afferent and feedback synapses in different ways, thus enhancing or suppressing information transmission (Hasselmo, 1999, 2006). Review articles emphasize that acetylcholine potentiates responses appropriate for environmental stimuli and decreases responses to stimuli that do not require immediate action (Picciotto, Higley, & Mineur, 2012). Gritton and colleagues (2016) suggest that cholinergic transients may play a pivotal role in synchronizing cortical neuronal output driven by salient cues to execute cue-guided responses. The exact mechanism that modifies synapses from the alpha center to the sensory areas is beyond the aim of the present article and is still hypothetical. This represents a testable prediction (see below), and it may be the subject of future model improvements. What is essential, for the moment, is that physiological mechanisms can support this model supposition.

Another fundamental assumption concerns the 180-degree shift between the alpha oscillation in the sensory (bottom) areas and the detection (top) centers. The idea that a suppression mechanism can be implemented by phase opposition of the alpha rhythm has been suggested by others recently (Bonnefond et al., 2017; Quax et al., 2017). Interestingly, much experimental data point out the role of the phase of the alpha rhythm in attention. Busch and colleagues (2009) observed that the oscillatory phase in the theta and alpha bands accounted for at least 16% of the variability in detection performance and allowed the prediction of performance in single trials. Mathewson, Gratton, Fabiani, Beck, and Ro (2009), using a masking paradigm, showed that the phase of the EEG alpha rhythm over posterior brain regions could reliably predict subsequent visual detection. Data from Fiebelkorn and colleagues (2013) also reveal that phase–detection relationships at higher frequencies are dependent on the phase of lower frequencies. A link between the prestimulus alpha phase and neural correlates of early visual perception was observed by Hülsdünker and colleagues (2018). Zhou, Iemi, Schoffelen, de Lange, and Haegens (2021) recently observed that both alpha power and alpha phase play a role in perception: Lower prestimulus alpha power in occipital-parietal areas improves perceptual sensitivity, whereas oscillatory alpha phase immediately before stimulus presentation modulates accuracy. Other authors, however, are more critical, suggesting that only the alpha amplitude but not the alpha phase is under top–down control (van Diepen & Mazaheri, 2018; van Diepen et al., 2015) or that the alpha phase is not involved in perception (Ruzzoli et al., 2019). However, the latter critics do not explicitly contradict our model. In fact, our model does not require the phase to be actively controlled in a top–down fashion. What is really controlled in our model is the amplitude of the alpha rhythm in the sensory region, which is under attentive top–down control. The model can work with any alpha phase, provided the two signals are generated with approximately 180 degrees of opposition. Of course, manipulating the phase in a sensory area, but not in the detection area, breaks this phase opposition and consequently affects the results.

Some experimental data support the idea of two alpha waves in phase opposition. Concerning the thalamus, the problem is discussed in Quax and colleagues (2017). These authors suggest that high-threshold thalamic cortical (TC) neurons can fire in a different phase than other thalamic neurons. Experimental data can be found in Lorincz, Kékesi, Juhász, Crunelli, and Hughes (2009). The authors demonstrated that, in the lateral geniculate nucleus, the presence of inhibitory interneurons enables the relay-mode TC neurons to form two distinct groups. One group exhibits cyclic suppression of firing during the negative peak of the α rhythm, whereas the other displays cyclic suppression during the positive peak.

In the Change to Unit 3: Two Antiphase Alpha Waves section, we propose a new model for Unit 3, which includes two populations of fast inhibitory interneurons and two populations of pyramidal neurons, along with a very fast excitatory link from pyramidal neurons to fast-GABAergic neurons (indicated with an orange line in Figure 10). This could be an α-amino-3-hydroxy-5-methyl-4-isoxazolepropionic acid (AMPA) excitatory synapse with very fast dynamics. In fact, analysis by fast application techniques indicates that AMPA receptors differ substantially in different types of neurons (Jonas, 2000). Interestingly, those with faster gating connect glutamatergic principal neurons to GABAergic interneurons (Geiger, Lübke, Roth, Frotscher, & Jonas, 1997; Hestrin, 1993) as in our schema. Measurements of excitatory postsynaptic currents in these synapses reveal decay time constants in the range of 1.3–2.0 msec or even lower (Jonas, 2000; Kleppe & Robinson, 1999; Geiger et al., 1997; Hestrin, 1993), allowing a submillisecond transmission at mature synapses (Cathala, Holderith, Nusser, DiGregorio, & Cull-Candy, 2005). These values are compatible with those required in our model of Figure 10, making the model physiologically reliable.

However, we are aware that the presence of two alpha waves in phase opposition has yet to be fully demonstrated and represents a testable prediction of the model.

Comparison with Previous Studies

The present model is indebted to several previous studies that have formulated similar assumptions. Some of them have already been described in the introduction. Here, we would like to highlight a few recent contributions that emphasize the role of the alpha rhythm phase. In the qualitative model by Jensen and colleagues (2012), alpha activity is conceived as peaks of inhibition, preventing

any firing. Only during a portion of the duty cycle, when this inhibition is reduced, can the most relevant stimuli be activated, according to a winner-take-all mechanism. Moreover, if the mean value and amplitude of the alpha wave are increased (see Figure 1 in that article), progressively less time remains available for excitation, and a reduced number of stimuli can be active. Hence, the level of alpha activity determines the number of neural representations that can be processed. This model, however, does not consider the phase difference among interconnected regions as an essential element for inhibition.

Quax and colleagues (2017) developed a model based on an idea more similar to the present one. They analyzed the behavior of two reciprocally interconnected neural populations of spiking neurons. They found that the phase difference between the alpha rhythms in the two populations strongly affects their communication, as evaluated by coherence in the gamma band. A further step in the same direction is provided by the qualitative model by Bonnefond and colleagues (2017). Assuming connectivity from Pool A to Pool B, the blocking of their communications can be due to two mechanisms: asynchrony in their low-frequency oscillatory activity (mainly in the alpha band) and the presence of strong alpha power in pool A, resulting in a shorter duty cycle. The same framework also assumes that alpha oscillations are internally controlled in terms of both amplitude and phase. The present model exploits a similar idea but utilizes a neural mass model of interconnected oscillating cortical regions, implementing a quantitative version within a comprehensive network (as opposed to just using two neurons). Remarkably, it demonstrates that the mechanism can be realized robustly and straightforwardly, assuming an on–off control of a few synapses (from the alpha generator to the sensory regions), which can reasonably be within an attentional control. To our knowledge, this is the first time a α-suppression mechanism is employed within a large network to address a general attention problem, demonstrating its practical feasibility and potential pathological implications.

Testable Predictions

Although, as documented above, all model assumptions can be found to have some neurophysiological counterparts in the literature, the mechanisms remain hypothetical, and some experiments can be devised to test the model's predictions and validate the main hypotheses.

The first fundamental prediction concerns variable synapses (from the alpha generator in the thalamus or pFC to the sensory regions) as a function of the attention task. This hypothesis can be tested by computing brain connectivity from fMRI data or high-density scalp EEG (with cortical reconstruction) during attention tasks. We predict that connectivity from the alpha generator (either the pulvinar or pFC) to the sensory area involved in the task increases when the stimulus in this area is suppressed. The same prediction can also be validated by studying the effect that certain neurotransmitters (such as acetylcholine and, more generally, the cholinergic system) have during attentional tasks, both in terms of selective neurotransmitter release in spatially localized areas and its impact on excitatory synapses. A second assumption of the model is that the alpha rhythm is in phase opposition when measured in a sensory area (where a distractor should be neglected) and in a cortical area devoted to processing of the information. Again, this prediction can be tested by measuring neural activity in different areas and computing the amplitude and phase of the oscillations in the alpha band. At a finer scale, local measurements of the alpha rhythm in thalamic or prefrontal neurons can reveal the existence of groups of neurons firing in opposition (as already partially documented by Lorincz et al., 2009), and the same phase can be observed in cortical areas differently involved in the task. Experiments can also be realized by disturbing the alpha phase in sensory areas during a task and comparing the effect of this maneuver with the one predicted by the model under analogous perturbed conditions. Finally, the model predicts that a deficit in gamma power and fast interneuron activity is reflected in attention deficits, which can also represent a further testable hypothesis, especially when correlated with similar aberrant attention in neurological patients, such as those with schizophrenia. A testable prediction is that reduced gamma activity is correlated with attention deficit.

Limitations and Future Work

In the present study, we have demonstrated one possible application of the proposed mechanism, specifically in the context of spatial attention, where stimuli originating from a particular portion of space can be suppressed through gamma–alpha superimposition. Interestingly, in this spatial model, additional nontrainable synapses are required in the sensory areas to implement a Gestalt proximity rule, in which the synapse strength decreases with distance. This is necessary to achieve gamma-band synchronization of all neurons coding for the same object. A proximity rule was used in the present work solely for simplicity. Of course, more complex rules (such as common fate, similarity, and good continuation) could be implemented in future work (see also La Cara & Ursino, 2008; Ursino & La Cara, 2004, for examples of a good continuation rule for the extraction of object contours).

In the present examples, we do not exploit a synchronization of the gamma oscillations within the detection units. In the first example, only one detection unit is used, whereas in the second, synchronization occurs in the sensory areas thanks to Gestalt proximity synapses. However, future model versions can also simulate more complex processing procedures in which synchronization occurs among units in the detection layer during the half-period of the alpha window. An example can be found in our previous models of semantic memory (Ursino & Pirazzini, 2023), which exploits a gamma rhythm to synchronize

different features of the same object in a high-level semantic area.

For the sake of simplicity, in this work, we assumed just ON/OFF control of alpha amplitude. Of course, in future work, it may be possible to continuously change the alpha amplitude (from a low level to a high level), introducing a more sophisticated modulation of attention.

The present model includes just four populations of neurons to represent a single oscillating Unit, that is, it implements minimal circuitry to demonstrate the feasibility of the proposed mechanism. More recent models (Wendling et al., 2024; Bensaid et al., 2019), based on current neurophysiological research, incorporate additional types of interneurons, account for key microcircuits at a cellular scale, and include communication among different cortical layers, representing the layered cytoarchitecture of neocortex. These models provide a more reliable description of neuroelectrical events. Of particular interest is the inclusion of vasoactive intestinal peptide interneurons in these models, which can play a crucial role in providing long-range disinhibition of pyramidal cells. Although we claim that the use of more complex neural architectures will not affect the substance of the present results, incorporating these improvements into future work will be of great value in enhancing the simulated neuroelectrical patterns and facilitating a more accurate comparison with EEG signals.

Additional improvements can concern a more detailed description of the alpha generator (as also hoped by Quax et al., 2017; but see also Figure 10), the simulation of multisensory effects or attention in semantic networks, and algorithms for a detailed side-by-side comparison between model behavior and neuroelectric data involving the alpha rhythm during attention tasks.

APPENDIX

Model Equations and Parameters

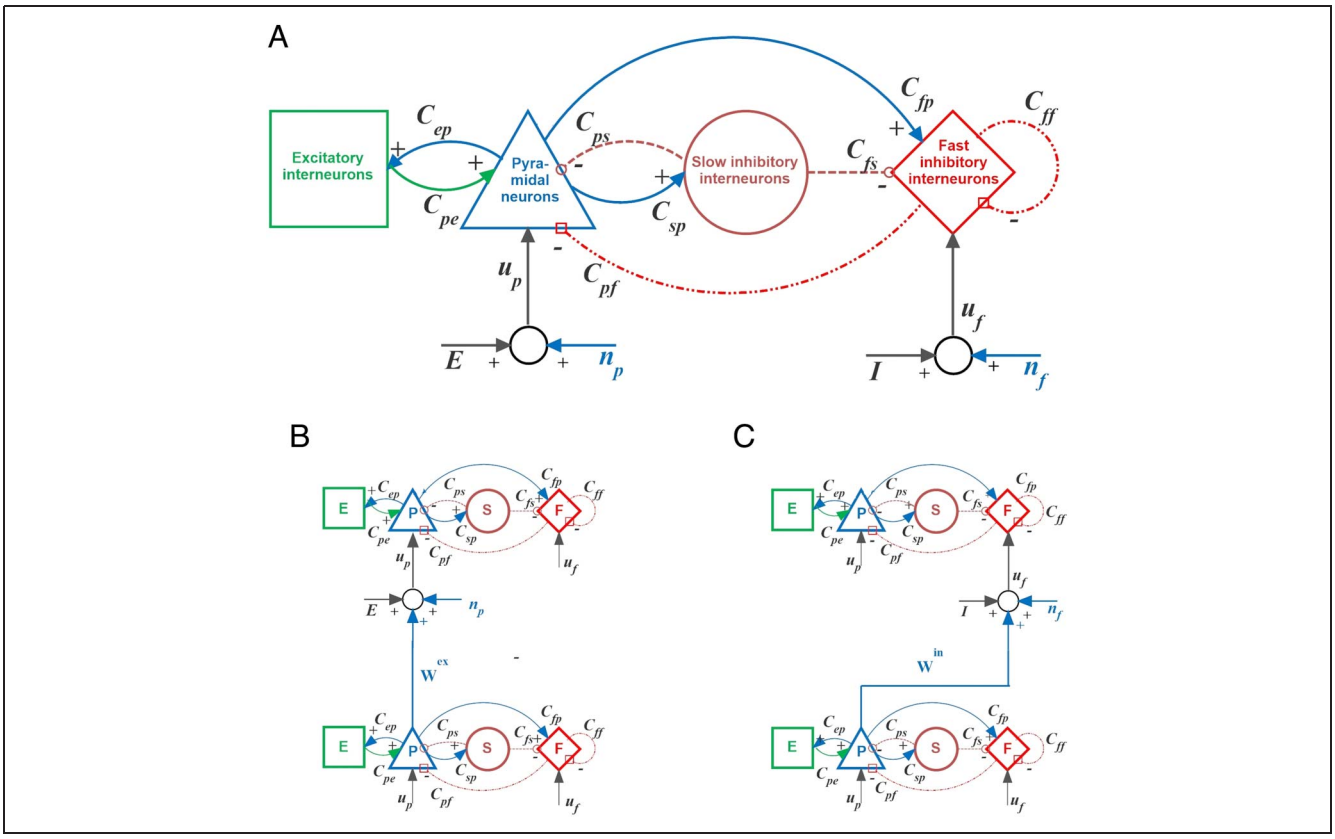

Figure A1. Upper column: (A) neural mass model simulating a single cortical column, the model's single computational unit. The dynamic results from the interaction among a population of pyramidal neurons, one of excitatory interneurons, and two populations of inhibitory interneurons with slow and fast synaptic dynamics, respectively. Continuous blue lines represent glutamatergic excitatory synapses. Brown dashed lines are GABAergic inhibitory synapses with slower dynamics, whereas red dash-dotted lines are GABAergic inhibitory synapses with faster dynamics. The constants C_{ij} represent internal connections among the populations, where the first subscript denotes the target population and the second subscript is the presynaptic population. E and I are external inputs to pyramidal neurons and fast inhibitory interneurons, respectively, whereas n_p and n_f represent white noise processed through a glutamatergic synapse. Bottom columns: two examples of connections among units. The left bottom figure (B) represents an excitatory connection (pyramidal to pyramidal) where W^{ex} is the connection strength. The right bottom figure (C) represents a disynaptic inhibitory connection (pyramidal – fast inhibitory – pyramidal) where W^{in} is the connection strength. In the last two figures, the symbols E and I represent the contribution of all other external synapses, excluding the indicated one.

Here, we present the model's equations, the training rules, and all related parameters.

Synapses

All synapses in the model are described by the following second order differential equation:

$$\frac{d^2y_n(t)}{dt^2} = \frac{G_n}{\tau_n} z_n(t) - \frac{2}{\tau_n}\frac{dy_n(t)}{dt} - \frac{y_n(t)}{\tau_n^2} \qquad (1)$$

where G_n is the gain, τ_n is the time constant, and z_n is the input to the synapse, that is, the presynaptic spike density. The subscript n is a generic one; it stands for either p, e, s, or f, depending on the neural population the equation is referring to: p for pyramidal neurons, e for excitatory interneurons, s for slow inhibitory interneurons, f for fast inhibitory interneurons. All second-order differential equations of type (1) are equivalent to the two first-order differential equations that follow.

$$\begin{cases} \dfrac{dy_n(t)}{dt} = x_n(t) \\ \dfrac{dx_n(t)}{dt} = \dfrac{G_n}{\tau_n} z_n(t) - \dfrac{2}{\tau_n} x_n(t) - \dfrac{y_n(t)}{\tau_n^2} \end{cases} \qquad (2)$$

Model of a Single Cortical Column

For each neuronal population, we first computed the mean membrane potential $v(t)$, which is influenced by synaptic connections. Then, we computed the average firing rate of the population, $z(t)$, through a sigmoidal activation function, $S(v(t))$. Finally, a normalized postsynaptic potential, $y(t)$, can be computed using the Equation 2; the latter must be multiplied by the synaptic weight to determine the actual contribution to the postsynaptic membrane potential.

Both pyramidal neurons and fast inhibitory interneurons can receive an external noise—labeled n_p and n_f, respectively. These are random variables with normal distribution, mean value m_p (or m_f), and standard deviation σ_p (or σ_f). Both reach the target population through an excitatory synapse. In the case of n_p, we implemented a common mathematical procedure to reduce the number of differential equations (and, therefore, the number of state variables). Specifically, we processed n_p through the excitatory synapse that goes from excitatory interneurons to pyramidal neurons (see Equation 4 below), instead of processing the input separately. The other external input, n_f, reaches its target population through a dedicated synapse (Equation 6).

The membrane potential of pyramidal neurons and fast inhibitory interneurons is also influenced by long-range synapses, which connect different cortical columns. Such contributions are labelled $E(t)$ and $I(t)$ and will be discussed in the next paragraph.

Equations for all populations.

Pyramidal neurons:

$$\begin{cases} v_p(t) = C_{pe}y_e(t) - C_{ps}y_s(t) - C_{pf}y_f(t) + E(t) \\ S(v_p(t)) = z_p(t) = \dfrac{2e_0}{1+e^{r(s_0-v_p)}} \\ \dfrac{dy_p(t)}{dt} = x_p(t) \\ \dfrac{dx_p(t)}{dt} = \dfrac{G_e}{\tau_e}z_p(t) - \dfrac{2}{\tau_e}x_p(t) - \dfrac{y_p(t)}{\tau_e^2} \end{cases} \quad (3)$$

Excitatory interneurons:

$$\begin{cases} v_e(t) = C_{ep}y_p(t) \\ S(v_e(t)) = z_e(t) = \dfrac{2e_0}{1+e^{r(s_0-v_e)}} \\ \dfrac{dy_e(t)}{dt} = x_e(t) \\ \dfrac{dx_e(t)}{dt} = \dfrac{G_e}{\tau_e}\left(z_e(t) + \dfrac{n_p}{C_{pe}}\right) - \dfrac{2}{\tau_e}x_e(t) - \dfrac{y_e(t)}{\tau_e^2} \end{cases} \quad (4)$$

Slow inhibitory interneurons:

$$\begin{cases} v_s(t) = C_{sp}y_p(t) \\ S(v_s(t)) = z_s(t) = \dfrac{2e_0}{1+e^{r(s_0-v_s)}} \\ \dfrac{dy_s(t)}{dt} = x_s(t) \\ \dfrac{dx_s(t)}{dt} = \dfrac{G_s}{\tau_s}z_s(t) - \dfrac{2}{\tau_s}x_s(t) - \dfrac{y_s(t)}{\tau_s^2} \end{cases} \quad (5)$$

Fast inhibitory interneurons:

$$\begin{cases} v_f(t) = C_{fp}y_p(t) - C_{fs}y_s(t) - C_{ff}y_f(t) + y_l(t) + I(t) \\ S(v_f(t)) = z_f(t) = \dfrac{2e_0}{1+e^{r(s_0-v_f(t))}} \\ \dfrac{dy_f(t)}{dt} = x_f(t) \\ \dfrac{dx_f(t)}{dt} = \dfrac{G_f}{\tau_f}z_f(t) - \dfrac{2}{\tau_f}x_f(t) - \dfrac{y_f(t)}{\tau_f^2} \\ \dfrac{dy_l(t)}{dt} = x_l(t) \\ \dfrac{dx_l(t)}{dt} = \dfrac{G_e}{\tau_e}(n_f(t)) - \dfrac{2}{\tau_e}x_l(t) - \dfrac{y_l(t)}{\tau_e^2} \end{cases} \quad (6)$$

where the subscript l is used to represent the quantities in the additional synapse, introduced to describe the effect of the noise n_f via glutamatergic dynamics. All related parameters' values are listed in the table below. Note that the variance of the noise is divided by the integration step, dt. In this way, we obtain a white noise with power density equal to $\sigma^2\,dt = 5$.

Long-range Connections

As previously mentioned, long-range synapses connect two different units, coding different features. These contributions appeared in the previous equations as the variables $E(t)$ and $I(t)$ (Equation 3 and Equation 6), which stand for long-range Excitation and long-range Inhibition, respectively.

In the following, we will use subscripts i to denote the position of a postsynaptic unit in the model and j for a

Table A1. Parameters Describing the Dynamics of the Populations within a Cortical Column, Generating the **Gamma Rhythm**

Synapses				*Function S(v(t))*	
G_e (mV)	5.17	τ_e (msec)	8	e_0 (Hz)	2.5
G_s (mV)	4.45	τ_s (msec)	33.33	r (mV^{-1})	0.56
G_f (mV)	57.1	τ_f (msec)	2.0	s_0 (mV)	15
Inputs		*Intracolumn Connections*			
m_p (Hz)	800 or 0	C_{ep}	54	C_{fp}	108
m_f (Hz)	0	C_{pe}	54	C_{fs}	27
σ_p^2 (s^{-2})	5/dt	C_{sp}	54	C_{pf}	300
σ_f^2 (s^{-2})	5/dt	C_{ps}	67.5	C_{ff}	10

Table A2. Parameters Describing the Dynamics of the Populations within a cortical Column, Generating the **Alpha Rhythm**

Synapses				*Function S(v(t))*	
G_e (mV)	5.17	τ_e (msec)	15.2	e_0 (Hz)	2.5
G_s (mV)	4.45	τ_s (msec)	23.8	r (mV^{-1})	0.56
G_f (mV)	57.1	τ_f (msec)	3.3	s_0 (mV)	15
Inputs		*Intracolumn Connections*			
m_p (Hz)	1000	C_{ep}	54	C_{fp}	35
m_f (Hz)	0	C_{pe}	54	C_{fs}	10
σ_p^2 (s^{-2})	5/dt	C_{sp}	54	C_{pf}	300
σ_f^2 (s^{-2})	5/dt	C_{ps}	450	C_{ff}	10

presynaptic unit. $E(t)$ and $I(t)$ are therefore calculated as follows:

Excitation:

$$E_i(t) = \sum_{i=1}^{N} W_{ij}^{ex} y_{p,j}(t - D_j) \tag{7}$$

Inhibition:

$$I_i(t) = \sum_{i=1}^{N} W_{ij}^{in} y_{p,j}(t - D_j) \tag{8}$$

where D_j represents the delay in the connectivity and N is the number of all presynaptic units. These delays were always assumed to be negligible, with the only exception being the delay from the alpha Unit to the sensory units, which implement a phase difference. The basal phase difference $\Delta\varphi = 2\pi D/T$, where T is the alpha period, was 165 degrees and was subject to a sensitivity analysis. Moreover, the delays internal to a spatial layer (see the "Spatial Gestalt Model" section) are assumed to be as high as 30 msec to favor gamma-band synchronization.

Models Used

The Simple Model

Synaptic weights among the populations:

$$W_{1\to4}^{ex} = 300 \quad W_{2\to4}^{ex} = 300 \quad W_{3\to1}^{in} = 0 \text{ or } W_{att}^{in}$$
$$W_{3\to2}^{in} = 0 \text{ or } W_{att}^{in} \quad W_{3\to4}^{in} = 100 \quad W_{att}^{in} = 100$$

Basal phase difference between 3→4 and 3→2 alpha connections: $\Delta\phi = 165$ degree.

The Spatial Gestalt Model

$$W_{L\to D}^{ex} = 400 \quad W_{R\to D}^{ex} = 400 \quad W_{alpba\to S}^{in} = 0 \text{ or } 100$$
$$W_{alpba\to D}^{in} = 100$$

Units in the left perception layer (and Units in the right one) are connected to implement a Gestalt proximity rule. These synapses decrease exponentially with the distance between the units:

$$W_{ij}^{ex} = W_{\max}^{ex} \exp\left(\frac{-d_{ij}^2}{2\sigma^2}\right)$$

$$W_{ij}^{in} = W_{\max}^{in} \exp\left(\frac{-d_{ij}^2}{2\sigma^2}\right) \tag{9}$$

where d_{ij} represents the spatial distance between units j and unit i in the same perception layer (left or right), $W_{\max}^{ex} = 140$, $W_{\max}^{in} = 100$ and $\sigma^2 = 0.7$. It is worth noting that both excitatory and inhibitory synapses are requested to improve synchronization.

Corresponding author: Mauro Ursino, Department of Electrical, Electronic, and Information Engineering "Guglielmo Marconi," Area di Campus Cesena, Via Dell'Università 50, I 47521 Cesena FC, Italy, e-mail: mauro.ursino@unibo.it.

Data Availability Statement

The MATLAB codes used for the analysis will be shared in the repository https://github.com/mauroursino/model_alpha_attention.git.

Author Contributions

Mauro Ursino: Conceptualization; Formal analysis; Funding acquisition; Investigation; Methodology; Software; Validation; Visualization; Writing—Original draft; Writing—Review & editing.

Funding Information

Work supported by #NEXTGENERATIONEU and funded by the Ministry of University and Research, National Recovery and Resilience Plan, project "A multiscale integrated approach to the study of the nervous system in health and disease" (MNESYS) (PE0000006)—a multiscale integrated approach to the study of the nervous system in health and disease (DN. 1553 11.10.2022).

Diversity in Citation Practices

Retrospective analysis of the citations in every article published in this journal from 2010 to 2021 reveals a persistent pattern of gender imbalance: Although the proportions of authorship teams (categorized by estimated gender identification of first author/last author) publishing in the *Journal of Cognitive Neuroscience* (*JoCN*) during this period were M(an)/M = .407, W(oman)/M = .32, M/W = .115, and W/W = .159, the comparable proportions for the articles that these authorship teams cited were M/M = .549, W/M = .257, M/W = .109, and W/W = .085 (Postle and Fulvio, *JoCN*, 34:1, pp. 1–3). Consequently, *JoCN* encourages all authors to consider gender balance explicitly when selecting which articles to cite and gives them the opportunity to report their article's gender citation balance.

REFERENCES

Alamia, A., Timmermann, C., Nutt, D. J., VanRullen, R., & Carhart-Harris, R. L. (2020). DMT alters cortical travelling waves. *eLife*, *9*, e59784. https://doi.org/10.7554/eLife.59784, PubMed: 33043883

Arana, L., Melcón, M., Kessel, D., Hoyos, S., Albert, J., Carretié, L., et al. (2022). Suppression of alpha-band power underlies exogenous attention to emotional distractors. *Psychophysiology*, *59*, e14051. https://doi.org/10.1111/psyp.14051, PubMed: 35318692

Bacigalupo, F., & Luck, S. J. (2022). Alpha-band EEG suppression as a neural marker of sustained attentional engagement to conditioned threat stimuli. *Social Cognitive and Affective Neuroscience*, *17*, 1101–1117. https://doi.org/10.1093/scan/nsac029, PubMed: 35434733

Barry, R. J., De Blasio, F. M., Fogarty, J. S., & Clarke, A. R. (2020). Natural alpha frequency components in resting EEG and their relation to arousal. *Clinical Neurophysiology*, *131*, 205–212. https://doi.org/10.1016/j.clinph.2019.10.018, PubMed: 31812081

Bensaid, S., Modolo, J., Merlet, I., Wendling, F., & Benquet, P. (2019). COALIA: A computational model of human EEG for consciousness research. *Frontiers in Systems Neuroscience*, *13*, 59. https://doi.org/10.3389/fnsys.2019.00059, PubMed: 31798421

Bonnefond, M., & Jensen, O. (2012). Alpha oscillations serve to protect working memory maintenance against anticipated distracters. *Current Biology*, *22*, 1969–1974. https://doi.org/10.1016/j.cub.2012.08.029, PubMed: 23041197

Bonnefond, M., & Jensen, O. (2013). The role of gamma and alpha oscillations for blocking out distraction. *Communicative & Integrative Biology*, *6*, e22702. https://doi.org/10.4161/cib.22702, PubMed: 23802042

Bonnefond, M., & Jensen, O. (2015). Gamma activity coupled to alpha phase as a mechanism for top–down controlled gating. *PLoS One*, *10*, e0128667. https://doi.org/10.1371/journal.pone.0128667, PubMed: 26039691

Bonnefond, M., Jensen, O., & Clausner, T. (2024). Visual processing by hierarchical and dynamic multiplexing. *eNeuro*, *11*, ENEURO.0282-24.2024. https://doi.org/10.1523/ENEURO.0282-24.2024, PubMed: 39537353

Bonnefond, M., Kastner, S., & Jensen, O. (2017). Communication between brain areas based on nested oscillations. *eNeuro*, *4*, ENEURO.0153-16.2017. https://doi.org/10.1523/ENEURO.0153-16.2017, PubMed: 28374013

Bourgeois, A., Guedj, C., Carrera, E., & Vuilleumier, P. (2020). Pulvino-cortical interaction: An integrative role in the control of attention. *Neuroscience and Biobehavioral Reviews*, *111*, 104–113. https://doi.org/10.1016/j.neubiorev.2020.01.005, PubMed: 31972202

Busch, N. A., Dubois, J., & VanRullen, R. (2009). The phase of ongoing EEG oscillations predicts visual perception. *Journal of Neuroscience*, *29*, 7869–7876. https://doi.org/10.1523/JNEUROSCI.0113-09.2009, PubMed: 19535598

Cantero, J. L., Atienza, M., Salas, R. M., & Gómez, C. M. (1999). Alpha EEG coherence in different brain states: An electrophysiological index of the arousal level in human subjects. *Neuroscience Letters*, *271*, 167–170. https://doi.org/10.1016/s0304-3940(99)00565-0, PubMed: 10507695

Cathala, L., Holderith, N. B., Nusser, Z., DiGregorio, D. A., & Cull-Candy, S. G. (2005). Changes in synaptic structure underlie the developmental speeding of AMPA receptor-mediated EPSCs. *Nature Neuroscience*, *8*, 1310–1318. https://doi.org/10.1038/nn1534, PubMed: 16172604

Chung, D. W., Geramita, M. A., & Lewis, D. A. (2022). Synaptic variability and cortical gamma oscillation power in schizophrenia. *American Journal of Psychiatry*, *179*, 277–287. https://doi.org/10.1176/appi.ajp.2021.21080798, PubMed: 35360919

Cona, F., & Ursino, M. (2015). A neural mass model of place cell activity: Theta phase precession, replay and imagination of never experienced paths. *Journal of Computational Neuroscience*, *38*, 105–127. https://doi.org/10.1007/s10827-014-0533-5, PubMed: 25284339

Cona, F., Zavaglia, M., Massimini, M., Rosanova, M., & Ursino, M. (2011). A neural mass model of interconnected regions simulates rhythm propagation observed via TMS-EEG. *Neuroimage*, *57*, 1045–1058. https://doi.org/10.1016/j.neuroimage.2011.05.007, PubMed: 21600291

Doesburg, S. M., Bedo, N., & Ward, L. M. (2016). Top–down alpha oscillatory network interactions during visuospatial attention orienting. *Neuroimage*, *132*, 512–519. https://doi.org/10.1016/j.neuroimage.2016.02.076, PubMed: 26952198

ElShafei, H. A., Bouet, R., Bertrand, O., & Bidet-Caulet, A. (2018). Two sides of the same coin: Distinct sub-bands in the α rhythm reflect facilitation and suppression mechanisms during auditory anticipatory attention. *eNeuro*, *5*, ENEURO.0141-18.2018. https://doi.org/10.1523/ENEURO.0141-18.2018, PubMed: 30225355

Ergenoglu, T., Demiralp, T., Bayraktaroglu, Z., Ergen, M., Beydagi, H., & Uresin, Y. (2004). Alpha rhythm of the EEG modulates visual detection performance in humans. *Cognitive Brain Research*, *20*, 376–383. https://doi.org/10.1016/j.cogbrainres.2004.03.009, PubMed: 15268915

Fiebelkorn, I. C., & Kastner, S. (2019). A rhythmic theory of attention. *Trends in Cognitive Sciences*, *23*, 87–101. https://doi.org/10.1016/j.tics.2018.11.009, PubMed: 30591373

Fiebelkorn, I. C., Saalmann, Y. B., & Kastner, S. (2013). Rhythmic sampling within and between objects despite sustained attention at a cued location. *Current Biology*, *23*, 2553–2558. https://doi.org/10.1016/j.cub.2013.10.063, PubMed: 24316204

Fiebelkorn, I. C., Snyder, A. C., Mercier, M. R., Butler, J. S., Molholm, S., & Foxe, J. J. (2013). Cortical cross-frequency coupling predicts perceptual outcomes. *Neuroimage*, *69*, 126–137. https://doi.org/10.1016/j.neuroimage.2012.11.021, PubMed: 23186917

Foster, J. J., & Awh, E. (2019). The role of alpha oscillations in spatial attention: Limited evidence for a suppression account. *Current Opinion in Psychology*, *29*, 34–40. https://doi.org/10.1016/j.copsyc.2018.11.001, PubMed: 30472541

Foxe, J. J., Simpson, G. V., & Ahlfors, S. P. (1998). Parieto-occipital approximately 10 Hz activity reflects anticipatory state of visual attention mechanisms. *NeuroReport*, *9*, 3929–3933. https://doi.org/10.1097/00001756-199812010-00030, PubMed: 9875731

Foxe, J. J., & Snyder, A. C. (2011). The role of alpha-band brain oscillations as a sensory suppression mechanism during selective attention. *Frontiers in Psychology*, *2*, 154. https://doi.org/10.3389/fpsyg.2011.00154, PubMed: 21779269

Fries, P. (2009). Neuronal gamma-band synchronization as a fundamental process in cortical computation. *Annual Review of Neuroscience*, *32*, 209–224. https://doi.org/10.1146/annurev.neuro.051508.135603, PubMed: 19400723

Fries, P. (2015). Rhythms for cognition: Communication through coherence. *Neuron*, *88*, 220–235. https://doi.org/10.1016/j.neuron.2015.09.034, PubMed: 26447583

Gaillard, C., & Ben Hamed, S. (2022). The neural bases of spatial attention and perceptual rhythms. *European Journal of Neuroscience*, *55*, 3209–3223. https://doi.org/10.1111/ejn.15044, PubMed: 33185294

Gaillard, C., Hadj Hassen, S. B., Di Bello, F., Bihan-Poudec, Y., VanRullen, R., & Hamed, S. B. (2020). Prefrontal attentional saccades explore space rhythmically. *Nature Communications*, *11*, 925. https://doi.org/10.1038/s41467-020-14649-7, PubMed: 32066740

Geiger, J. R., Lübke, J., Roth, A., Frotscher, M., & Jonas, P. (1997). Submillisecond AMPA receptor-mediated signaling at a principal neuron–interneuron synapse. *Neuron*, *18*, 1009–1023. https://doi.org/10.1016/s0896-6273(00)80339-6, PubMed: 9208867

Gerfen, C. R., Economo, M. N., & Chandrashekar, J. (2018). Long distance projections of cortical pyramidal neurons. *Journal of Neuroscience Research*, *96*, 1467–1475. https://doi.org/10.1002/jnr.23978, PubMed: 27862192

Grent-'t-Jong, T., Gross, J., Goense, J., Wibral, M., Gajwani, R., Gumley, A. I., et al. (2018). Resting-state gamma-band power alterations in schizophrenia reveal E/I-balance abnormalities across illness-stages. *eLife*, *7*, e37799. https://doi.org/10.7554/eLife.37799, PubMed: 30260771

Gritton, H. J., Howe, W. M., Mallory, C. S., Hetrick, V. L., Berke, J. D., & Sarter, M. (2016). Cortical cholinergic signaling controls the detection of cues. *Proceedings of the National Academy of Sciences, U.S.A.*, *113*, E1089–E1097. https://doi.org/10.1073/pnas.1516134113, PubMed: 26787867

Halgren, M., Ulbert, I., Bastuji, H., Fabó, D., Erőss, L., Rey, M., et al. (2019). The generation and propagation of the human alpha rhythm. *Proceedings of the National Academy of Sciences, U.S.A.*, *116*, 23772–23782. https://doi.org/10.1073/pnas.1913092116, PubMed: 31685634

Harris, A. M., Dux, P. E., & Mattingley, J. B. (2018). Detecting unattended stimuli depends on the phase of prestimulus neural oscillations. *Journal of Neuroscience*, *38*, 3092–3101. https://doi.org/10.1523/JNEUROSCI.3006-17.2018, PubMed: 29459372

Hasenstaub, A., Shu, Y., Haider, B., Kraushaar, U., Duque, A., & McCormick, D. A. (2005). Inhibitory postsynaptic potentials carry synchronized frequency information in active cortical networks. *Neuron*, *47*, 423–435. https://doi.org/10.1016/j.neuron.2005.06.016, PubMed: 16055065

Hasselmo, M. E. (1999). Neuromodulation: Acetylcholine and memory consolidation. *Trends in Cognitive Sciences*, *3*, 351–359. https://doi.org/10.1016/s1364-6613(99)01365-0, PubMed: 10461198

Hasselmo, M. E. (2006). The role of acetylcholine in learning and memory. *Current Opinion in Neurobiology*, *16*, 710–715. https://doi.org/10.1016/j.conb.2006.09.002, PubMed: 17011181

Hasselmo, M. E., & Giocomo, L. M. (2006). Cholinergic modulation of cortical function. *Journal of Molecular Neuroscience*, *30*, 133–135. https://doi.org/10.1385/JMN:30:1:133, PubMed: 17192659

Hestrin, S. (1993). Different glutamate receptor channels mediate fast excitatory synaptic currents in inhibitory and excitatory cortical neurons. *Neuron*, *11*, 1083–1091. https://doi.org/10.1016/0896-6273(93)90221-c, PubMed: 7506044

Hülsdünker, T., Strüder, H. K., & Mierau, A. (2018). The pre-stimulus oscillatory alpha phase affects neural correlates of early visual perception. *Neuroscience Letters*, *685*, 90–95. https://doi.org/10.1016/j.neulet.2018.08.020, PubMed: 30130554

Iemi, L., Chaumon, M., Crouzet, S. M., & Busch, N. A. (2017). Spontaneous neural oscillations bias perception by modulating baseline excitability. *Journal of Neuroscience*, *37*, 807–819. https://doi.org/10.1523/JNEUROSCI.1432-16.2016, PubMed: 28123017

Ikkai, A., Dandekar, S., & Curtis, C. E. (2016). Lateralization in alpha-band oscillations predicts the locus and spatial distribution of attention. *PLoS One*, *11*, e0154796. https://doi.org/10.1371/journal.pone.0154796, PubMed: 27144717

Jansen, B. H., & Rit, V. G. (1995). Electroencephalogram and visual evoked potential generation in a mathematical model of coupled cortical columns. *Biological Cybernetics*, *73*, 357–366. https://doi.org/10.1007/BF00199471, PubMed: 7578475

Janssens, C., De Loof, E., Boehler, C. N., Pourtois, G., & Verguts, T. (2018). Occipital alpha power reveals fast attentional inhibition of incongruent distractors. *Psychophysiology*, *55* https://doi.org/10.1111/psyp.13011, PubMed: 28929499

Jensen, O., Bonnefond, M., & VanRullen, R. (2012). An oscillatory mechanism for prioritizing salient unattended stimuli. *Trends in Cognitive Sciences*, *16*, 200–206. https://doi.org/10.1016/j.tics.2012.03.002, PubMed: 22436764

Jensen, O., Gips, B., Bergmann, T. O., & Bonnefond, M. (2014). Temporal coding organized by coupled alpha and gamma oscillations prioritize visual processing. *Trends in Neurosciences*, *37*, 357–369. https://doi.org/10.1016/j.tins.2014.04.001, PubMed: 24836381

Jonas, P. (2000). The time course of signaling at central glutamatergic synapses. *News in Physiological Sciences*, *15*, 83–89. https://doi.org/10.1152/physiologyonline.2000.15.2.83, PubMed: 11390884

Kaas, J. H., & Lyon, D. C. (2007). Pulvinar contributions to the dorsal and ventral streams of visual processing in primates. *Brain Research Reviews*, *55*, 285–296. https://doi.org/10.1016/j.brainresrev.2007.02.008, PubMed: 17433837

Karvat, G., & Landau, A. N. (2024). A role for bottom–up alpha oscillations in temporal integration. *Journal of Cognitive Neuroscience*, *36*, 632–639. https://doi.org/10.1162/jocn_a_02056, PubMed: 37713671

Kleppe, I. C., & Robinson, H. P. (1999). Determining the activation time course of synaptic AMPA receptors from openings of colocalized NMDA receptors. *Biophysical Journal*, *77*, 1418–1427. https://doi.org/10.1016/S0006-3495(99)76990-0, PubMed: 10465753

Klimesch, W. (2012). α-band oscillations, attention, and controlled access to stored information. *Trends in Cognitive Sciences*, *16*, 606–617. https://doi.org/10.1016/j.tics.2012.10.007, PubMed: 23141428

La Cara, G.-E., & Ursino, M. (2008). A model of contour extraction including multiple scales, flexible inhibition and attention. *Neural Networks*, *21*, 759–773. https://doi.org/10.1016/j.neunet.2007.11.003, PubMed: 18406105

Lakatos, P., O'Connell, M. N., & Barczak, A. (2016). Pondering the pulvinar. *Neuron*, *89*, 5–7. https://doi.org/10.1016/j.neuron.2015.12.022, PubMed: 26748085

Lewis, D. A., Curley, A. A., Glausier, J. R., & Volk, D. W. (2012). Cortical parvalbumin interneurons and cognitive dysfunction in schizophrenia. *Trends in Neurosciences*, *35*, 57–67. https://doi.org/10.1016/j.tins.2011.10.004, PubMed: 22154068

Limbach, K., & Corballis, P. M. (2016). Prestimulus alpha power influences response criterion in a detection task. *Psychophysiology*, *53*, 1154–1164. https://doi.org/10.1111/psyp.12666, PubMed: 27144476

Lorincz, M. L., Kékesi, K. A., Juhász, G., Crunelli, V., & Hughes, S. W. (2009). Temporal framing of thalamic relay-mode firing by phasic inhibition during the alpha rhythm. *Neuron*, *63*, 683–696. https://doi.org/10.1016/j.neuron.2009.08.012, PubMed: 19755110

Lundqvist, M., Herman, P., & Lansner, A. (2013). Effect of prestimulus alpha power, phase, and synchronization on stimulus detection rates in a biophysical attractor network model. *Journal of Neuroscience*, *33*, 11817–11824. https://doi.org/10.1523/JNEUROSCI.5155-12.2013, PubMed: 23864671

Marín, O. (2012). Interneuron dysfunction in psychiatric disorders. *Nature Reviews Neuroscience*, *13*, 107–120. https://doi.org/10.1038/nrn3155, PubMed: 22251963

Mathewson, K. E., Beck, D. M., Ro, T., Maclin, E. L., Low, K. A., Fabiani, M., et al. (2014). Dynamics of alpha control: Preparatory suppression of posterior alpha oscillations by frontal modulators revealed with combined EEG and event-related optical signal. *Journal of Cognitive Neuroscience*, *26*, 2400–2415. https://doi.org/10.1162/jocn_a_00637, PubMed: 24702458

Mathewson, K. E., Gratton, G., Fabiani, M., Beck, D. M., & Ro, T. (2009). To see or not to see: Prestimulus alpha phase predicts visual awareness. *Journal of Neuroscience*, *29*, 2725–2732. https://doi.org/10.1523/JNEUROSCI.3963-08.2009, PubMed: 19261866

Mishra, J., Lowenstein, M., Campusano, R., Hu, Y., Diaz-Delgado, J., Ayyoub, J., et al. (2021). Closed-loop neurofeedback of α synchrony during goal-directed attention. *Journal of Neuroscience*, *41*, 5699–5710. https://doi.org/10.1523/JNEUROSCI.3235-20.2021, PubMed: 34021043

Misselhorn, J., Friese, U., & Engel, A. K. (2019). Frontal and parietal alpha oscillations reflect attentional modulation of cross-modal matching. *Scientific Reports*, *9*, 5030. https://doi.org/10.1038/s41598-019-41636-w, PubMed: 30903012

Nakazawa, K., Zsiros, V., Jiang, Z., Nakao, K., Kolata, S., Zhang, S., et al. (2012). GABAergic interneuron origin of schizophrenia pathophysiology. *Neuropharmacology*, *62*, 1574–1583. https://doi.org/10.1016/j.neuropharm.2011.01.022, PubMed: 21277876

Peylo, C., Hilla, Y., & Sauseng, P. (2021). Cause or consequence? Alpha oscillations in visuospatial attention. *Trends in Neurosciences*, *44*, 705–713. https://doi.org/10.1016/j.tins.2021.05.004, PubMed: 34167840

Pfurtscheller, G., Stancák, A., Jr., & Neuper, C. (1996). Event-related synchronization (ERS) in the alpha band—An electrophysiological correlate of cortical idling: A review. *International Journal of Psychophysiology*, *24*, 39–46. https://doi.org/10.1016/S0167-8760(96)00066-9, PubMed: 8978434

Picciotto, M. R., Higley, M. J., & Mineur, Y. S. (2012). Acetylcholine as a neuromodulator: Cholinergic signaling shapes nervous system function and behavior. *Neuron*, *76*, 116–129. https://doi.org/10.1016/j.neuron.2012.08.036, PubMed: 23040810

Popov, T., Kastner, S., & Jensen, O. (2017). FEF-controlled alpha delay activity precedes stimulus-induced gamma-band activity in visual cortex. *Journal of Neuroscience*, *37*, 4117–4127. https://doi.org/10.1523/JNEUROSCI.3015-16.2017, PubMed: 28314817

Prodöhl, C., Würtz, R. P., & von der Malsburg, C. (2003). Learning the Gestalt rule of collinearity from object motion. *Neural Computation*, *15*, 1865–1896. https://doi.org/10.1162/08997660360675071, PubMed: 14511516

Quax, S., Jensen, O., & Tiesinga, P. (2017). Top–down control of cortical gamma-band communication via pulvinar induced phase shifts in the alpha rhythm. *PLoS Computational Biology*, *13*, e1005519. https://doi.org/10.1371/journal.pcbi.1005519, PubMed: 28472057

Raposo, I., Szczepanski, S. M., Haaland, K., Endestad, T., Solbakk, A.-K., Knight, R. T., et al. (2023). Periodic attention deficits after frontoparietal lesions provide causal evidence for rhythmic attentional sampling. *Current Biology*, *33*, 4893–4904. https://doi.org/10.1016/j.cub.2023.09.065, PubMed: 37852264

Ricci, G., Magosso, E., & Ursino, M. (2021). The relationship between oscillations in brain regions and functional connectivity: A critical analysis with the aid of neural mass models. *Brain Sciences*, *11*, 487. https://doi.org/10.3390/brainsci11040487, PubMed: 33921414

Ruzzoli, M., Torralba, M., Morís Fernández, L., & Soto-Faraco, S. (2019). The relevance of alpha phase in human perception. *Cortex*, *120*, 249–268. https://doi.org/10.1016/j.cortex.2019.05.012, PubMed: 31352236

Salkoff, D. B., Zagha, E., Yüzgeç, Ö., & McCormick, D. A. (2015). Synaptic mechanisms of tight spike synchrony at gamma frequency in cerebral cortex. *Journal of Neuroscience*, *35*, 10236–10251. https://doi.org/10.1523/JNEUROSCI.0828-15.2015, PubMed: 26180200

Samaha, J., Bauer, P., Cimaroli, S., & Postle, B. R. (2015). Top–down control of the phase of alpha-band oscillations as a mechanism for temporal prediction. *Proceedings of the National Academy of Sciences, U.S.A.*, *112*, 8439–8444. https://doi.org/10.1073/pnas.1503686112, PubMed: 26100913

Schmid, M. C., Singer, W., & Fries, P. (2012). Thalamic coordination of cortical communication. *Neuron*, *75*, 551–552. https://doi.org/10.1016/j.neuron.2012.08.009, PubMed: 22920248

Schneider, D., Herbst, S. K., Klatt, L.-I., & Wöstmann, M. (2022). Target enhancement or distractor suppression? Functionally distinct alpha oscillations form the basis of attention. *European Journal of Neuroscience*, *55*, 3256–3265. https://doi.org/10.1111/ejn.15309, PubMed: 33973310

Senkowski, D., & Gallinat, J. (2015). Dysfunctional prefrontal gamma-band oscillations reflect working memory and other cognitive deficits in schizophrenia. *Biological Psychiatry*, *77*, 1010–1019. https://doi.org/10.1016/j.biopsych.2015.02.034, PubMed: 25847179

Shipp, S. (2003). The functional logic of cortico–pulvinar connections. *Philosophical Transactions of the Royal Society of London, Series B: Biological Sciences*, *358*, 1605–1624. https://doi.org/10.1098/rstb.2002.1213, PubMed: 14561322

Sun, Y., Farzan, F., Barr, M. S., Kirihara, K., Fitzgerald, P. B., Light, G. A., et al. (2011). γ oscillations in schizophrenia: Mechanisms and clinical significance. *Brain Research*, *1413*, 98–114. https://doi.org/10.1016/j.brainres.2011.06.065, PubMed: 21840506

Tabarelli, D., Brancaccio, A., Zrenner, C., & Belardinelli, P. (2022). Functional connectivity states of alpha rhythm sources in the human cortex at rest: Implications for real-time brain state dependent EEG-TMS. *Brain Sciences*, *12*, 348. https://doi.org/10.3390/brainsci12030348, PubMed: 35326304

Ursino, M., Cesaretti, N., & Pirazzini, G. (2023). A model of working memory for encoding multiple items and ordered

sequences exploiting the theta-gamma code. *Cognitive Neurodynamics*, *17*, 489–521. https://doi.org/10.1007/s11571-022-09836-9, PubMed: 37007198
Ursino, M., Cona, F., & Zavaglia, M. (2010). The generation of rhythms within a cortical region: Analysis of a neural mass model. *Neuroimage*, *52*, 1080–1094. https://doi.org/10.1016/j.neuroimage.2009.12.084, PubMed: 20045071
Ursino, M., & La Cara, G. E. (2004). A model of contextual interactions and contour detection in primary visual cortex. *Neural Networks*, *17*, 719–735. https://doi.org/10.1016/j.neunet.2004.03.007, PubMed: 15288894
Ursino, M., Magosso, E., & Cuppini, C. (2009). Recognition of abstract objects via neural oscillators: Interaction among topological organization, associative memory and gamma band synchronization. *IEEE Transactions on Neural Networks*, *20*, 316–335. https://doi.org/10.1109/TNN.2008.2006326, PubMed: 19171515
Ursino, M., Magosso, E., La Cara, G.-E., & Cuppini, C. (2006). Object segmentation and recovery via neural oscillators implementing the similarity and prior knowledge gestalt rules. *Biosystems*, *85*, 201–218. https://doi.org/10.1016/j.biosystems.2006.01.005, PubMed: 16635545
Ursino, M., & Pirazzini, G. (2023). Construction of a hierarchical organization in semantic memory: A model based on neural masses and gamma-band synchronization. *Cognitive Computation*, *16*, 326–347. https://doi.org/10.1007/s12559-023-10202-y
van Diepen, R. M., Cohen, M. X., Denys, D., & Mazaheri, A. (2015). Attention and temporal expectations modulate power, not phase, of ongoing alpha oscillations. *Journal of Cognitive Neuroscience*, *27*, 1573–1586. https://doi.org/10.1162/jocn_a_00803, PubMed: 25774428
van Diepen, R. M., Foxe, J. J., & Mazaheri, A. (2019). The functional role of alpha-band activity in attentional processing: The current zeitgeist and future outlook. *Current Opinion in Psychology*, *29*, 229–238. https://doi.org/10.1016/j.copsyc.2019.03.015, PubMed: 31100655
van Diepen, R. M., & Mazaheri, A. (2018). The caveats of observing inter-trial phase-coherence in cognitive neuroscience. *Scientific Reports*, *8*, 2990. https://doi.org/10.1038/s41598-018-20423-z, PubMed: 29445210
van Dijk, H., Schoffelen, J.-M., Oostenveld, R., & Jensen, O. (2008). Prestimulus oscillatory activity in the alpha band predicts visual discrimination ability. *Journal of Neuroscience*, *28*, 1816–1823. https://doi.org/10.1523/JNEUROSCI.1853-07.2008, PubMed: 18287498
Viriyopase, A., Memmesheimer, R.-M., & Gielen, S. (2016). Cooperation and competition of gamma oscillation mechanisms. *Journal of Neurophysiology*, *116*, 232–251. https://doi.org/10.1152/jn.00493.2015, PubMed: 26912589
Wendling, F., Bartolomei, F., Bellanger, J. J., & Chauvel, P. (2002). Epileptic fast activity can be explained by a model of impaired GABAergic dendritic inhibition. *European Journal of Neuroscience*, *15*, 1499–1508. https://doi.org/10.1046/j.1460-9568.2002.01985.x, PubMed: 12028360
Wendling, F., Koksal-Ersoz, E., Al-Harrach, M., Yochum, M., Merlet, I., Ruffini, G., et al. (2024). Multiscale neuro-inspired models for interpretation of EEG signals in patients with epilepsy. *Clinical Neurophysiology*, *161*, 198–210. https://doi.org/10.1016/j.clinph.2024.03.006, PubMed: 38520800
Wildegger, T., van Ede, F., Woolrich, M., Gillebert, C. R., & Nobre, A. C. (2017). Preparatory α-band oscillations reflect spatial gating independently of predictions regarding target identity. *Journal of Neurophysiology*, *117*, 1385–1394. https://doi.org/10.1152/jn.00856.2016, PubMed: 28077669
Wöstmann, M., Alavash, M., & Obleser, J. (2019). Alpha oscillations in the human brain implement distractor suppression independent of target selection. *Journal of Neuroscience*, *39*, 9797–9805. https://doi.org/10.1523/JNEUROSCI.1954-19.2019, PubMed: 31641052
Zazio, A., Schreiber, M., Miniussi, C., & Bortoletto, M. (2020). Modelling the effects of ongoing alpha activity on visual perception: The oscillation-based probability of response. *Neuroscience & Biobehavioral Reviews*, *112*, 242–253. https://doi.org/10.1016/j.neubiorev.2020.01.037, PubMed: 32023485
Zhou, Y. J., Iemi, L., Schoffelen, J.-M., de Lange, F. P., & Haegens, S. (2021). Alpha oscillations shape sensory representation and perceptual sensitivity. *Journal of Neuroscience*, *41*, 9581–9592. https://doi.org/10.1523/JNEUROSCI.1114-21.2021, PubMed: 34593605